Hypoxia is a characteristic feature of many solid tumors; it affects every major aspect of cancer biology, including cell invasion, recurrence, and metastasis.[10] In several cancers, poor prognosis is closely related to intratumoral hypoxia and/or expression of hypoxia-related endogenous proteins, including vascular endothelial growth factor, hypoxia-inducible factor-1, and glucose transporter 1.[11–16] It has been noted that, although hypoxia kills most tumor cells, it provides strong selective pressure for survival of the most aggressive and metastatic cells.[17] These cells proficiently escape the noxious hypoxic microenvironment by activating an invasive epithelial–mesenchymal transition (EMT), inducing angiogenesis, and promoting other metastatic programs that ultimately lead to tumor recurrence or metastasis.[18–23] In addition, hypoxia-inducible gene expression profiles have been associated with poor prognosis in human cancers.[23] Taken together, these data suggested that hypoxic conditions significantly affect HCC; however, it is unclear which hypoxia-inducible genes are most significantly related to HCC.[24]

We previously studied microarray data of liver metastases from colorectal cancer to identify hypoxia-inducible genes.[25] Of the 3,000 genes ranked in the microarray data, the top 30 were identified as hypoxia-inducible genes. Among the 30 genes, we focused on a histone H3, lysine 9 demethylase known as Jumonji domain containing 1A (JMJD1A). We showed that JMJD1A expression was a novel, independent, prognostic marker for colorectal cancer.[25] The functional relevance of JMJD1A has not been fully clarified, but it appears to cause transcriptional activation of various downstream target genes and amplifies hypoxia-inducible gene expression.[26–29] We confirmed that JMJD1A was induced in three HCC cell lines under hypoxic conditions. We hypothesized that JMJD1A was a significant gene activator and switch for an epigenetic pathway in hypoxic conditions; furthermore, JMJD1A expression may serve as a prognostic marker for HCC.

In this study, we aim to confirm the expression and localization of JMJD1A and assess its potential as a prognostic indicator in HCC by comparing its expression in HCC and liver background tissues. Moreover, we performed JMJD1A suppression analysis to determine whether JMJD1A might play a role in increasing the malignant potency of HCC cells under hypoxic conditions.

MATERIALS AND METHODS

Cell Lines and Culture

Human HCC cell lines (HuH7, PLC/PRF/5[PLC], and HepG2) were obtained from the Japan Cancer Research Resources Bank (Osaka, Japan). Cells were grown in Dulbecco's modified Eagle's medium supplemented with 10% fetal bovine serum, and 100 units/ml penicillin at 37°C in a humidified incubator with 5% CO_2. For hypoxic conditions, cells were grown for up to 72 h at 37°C in a continuously monitored atmosphere of 1% O2, 5% CO_2, and 94% N_2 in a multigas incubator (model 9200; Wakenyaku Co., Kyoto, Japan). Control/reference cells were cultured in normoxic conditions (21% O_2).

Clinical Samples

A total of 110 quality-verified HCC samples and paired noncancerous samples were obtained from patients who underwent liver resection from 2000 to 2005 at Osaka University Hospital. All patients were clearly diagnosed with HCC, based on clinicopathological findings. Mean age was 63.4 ± 0.9 years; male-to-female ratio was 89:21; tumor size was 5.1 ± 0.3 cm; and mean follow-up time was 32.6 ± 3.3 months. Patient clinicopathological features are presented in Table 2. During surgery, HCC and corresponding noncancerous tissue samples were immediately suspended in an RNA stabilization reagent (RNA Later; Ambion, Inc., Austin, TX) and stored at –80°C until RNA extraction. Other resected HCC specimens were preserved in paraffin blocks. The use of resected samples was approved by the Human Ethics Review Committee of the Graduate School of Medicine, Osaka University, and informed consent was obtained from each patient included in the study.

Immunohistochemistry

Immunohistochemical studies of JMJD1A were performed on 87 surgical specimens of HCC, as described previously.[30] Briefly, formalin-fixed, paraffin-embedded tissues were deparaffinized, microwaved for antigen retrieval, incubated with specific, rabbit polyclonal, anti-JMJD1A antibodies (1:100 dilution; Proteintech Group, Inc., Chicago, IL) for 1 h at room temperature, and detected with avidin–biotin complex reagents (Vector Laboratory Inc., Burlingame, CA) and diaminobenzidine. All sections were counterstained with hematoxylin. For negative controls, the primary antibody was substituted with nonimmunized immunoglobulin G (Vector Laboratories)

Western Blot Analysis

Western blot analysis was performed as described previously.[31] Briefly, total protein was extracted from HCC cell lines in radio immunoprecipitation assay (RIPA) buffer (Thermo Fisher Scientific, Inc., Rockford, IL). Aliquots of total protein (12 μg) were electrophoresed on sodium dodecyl sulfate polyacrylamide gel electrophoresis (SDS-PAGE), 10% Tris-HCl gels (Bio-Rad Laboratories Inc.,

Hercules, CA). The separated proteins were transferred to polyvinylidene difluoride membranes (Millipore Co., Billerica, MA) and incubated with primary antibodies for 1 h. Proteins were detected with the anti-JMJD1A antibody (diluted 1:800) and anti β-actin antibody (diluted 1:1,000; Sigma, Co., Tokyo, Japan).

qRT-PCR

Total RNA was isolated from cultured cells or tumor tissues with Trizol reagent (Invitrogen, Carlsbad, CA, USA) as previously described.[32] Complementary DNA was synthesized from 8.0 μg total RNA with the SuperScript first-strand synthesis system (Invitrogen), according to the manufacturer's protocol.

Real-time quantitative polymerase chain reactions (qRT-PCR) were conducted with the LightCycler-FastStart DNA Master SYBR Green I kit (Roche Applied Science) with the gene-specific oligonucleotide primers presented in Table 1.[25,30,32–34] Amplifications were performed in triplicate with the LightCycler system (Roche Applied Science, Indianapolis, IN) and the following protocol: initial denaturation at 95°C for10 min, followed by 45 cycles of 95°C for 10 s, 55°C for 10 s, and 60°C for 10 s. Melting curve analysis was performed to distinguish specific products from nonspecific products and primer dimers. Relative expression was calculated as the ratio of specific messenger RNA (mRNA) to endogenous β-actin mRNA in each sample.

Transfection of Small Interfering RNA (siRNA)

For siRNA suppression, we used a Stealth RNAi kit (Invitrogen, Carlsbad, CA) with double-stranded RNA duplexes that targeted human JMJD1A, (5-AGAAGA AUUCAAGAGAUUCCGGAGG-3/5-CCUCCGGAAUCU CUUGAAUUCUUCU-3), and negative control siRNA (NC), as previously described.[25] HCC cell lines were transfected with the siRNAs in lipofectamine RNAiMAX (Invitrogen), according to the manufacturer's protocols.

Proliferation and Invasion Assays

The proliferation assay was performed with a Cell Counting Kit-8 (Dojindo Molecular Technologies, Rockville, MD), as described previously.[35] Briefly, the viable cell number was determined by the absorbance value. We calculated the ratios of day 0 absorbance to day 1, 2 or 3 absorbance values. The invasion assay was performed with Transwell cell culture chambers (BD Biosciences, Bedford, MA), as described previously.[36] Briefly, 5×10^5 cells were seeded in triplicate on a Matrigel-coated membrane. After 48 h, cells that had invaded the undersurface of the membrane were fixed with 100% methanol and stained with 1% toluidine blue. Four microscopic fields were randomly selected for cell counting.

Statistical Analysis

Statistical analysis was performed with Student's *t*-test or Fisher's exact test for categorical data and the Mann–Whitney *U* test for nonparametric data. Correlation significance was assessed with Pearson's correlation coefficient test. Receiver operating characteristic (ROC) curves were established by plotting positive versus (1—negative) immunohistochemical samples. The Youden index (sensitivity + specificity − 1) was used to determine the optimal cutoff point for JMJD1A mRNA levels to predict disease-free survival.[37] The Kaplan–Meier analysis and the log-rank test were used to construct the disease-free survival curve and to evaluate differences. The prognostic value of each clinicopathologic characteristic was first determined by univariate Cox regression analysis. Parameters significantly related to survival on univariate analysis were included in multivariate analysis to identify significant clinicopathologic factors. *P*-values < 0.05 were considered statistically significant. All statistical analysis was carried out with JMP 8.0 software (SAS Institute, Tokyo, Japan).

RESULTS

Relationship between JMJD1A mRNA and Protein Expression

JMJD1A mRNA expression was significantly higher in HCC tissues ($1.03 \pm 2.67 \times 10^7$, mean ± SD; 2.82, median; $n = 110$) than in corresponding noncancerous tissues (0.133 ± 0.027; 0.119; $n = 21$) (Fig. 1a, $P < 0.0001$). JMJD1A protein expression was observed in 26 of 87 HCC

TABLE 1 Primers used for RT-PCR assay

Gene	Sense primer	Antisense primer
JMJD1A	5′-GCAAAGGACACGGAGAAGAT-3′	5′-CCCAGCCTTGAACTCCATAC-3′
E-cadherin	5′-TGCCCAGAAAATGAAAAAGG-3′	5′-GTGTATGTGGCAATGCGTTC-3′
N-cadherin	5′-TGAAACGCCGGGATAAAGAACG-3′	5′-TGCTGCAGCTGGCTCAAGTCAT-3′
Twist	5′-GGGAGTCCGCAGTCTTACGA-3′	5′-AGACCGAGAAGGCGTAGCTG-3′
β-Actin	5′-TTGTTACAGGAAGTCCCTTGCC-3′	5′-ATGCTATCACCTCCCCTGTGTG-3′

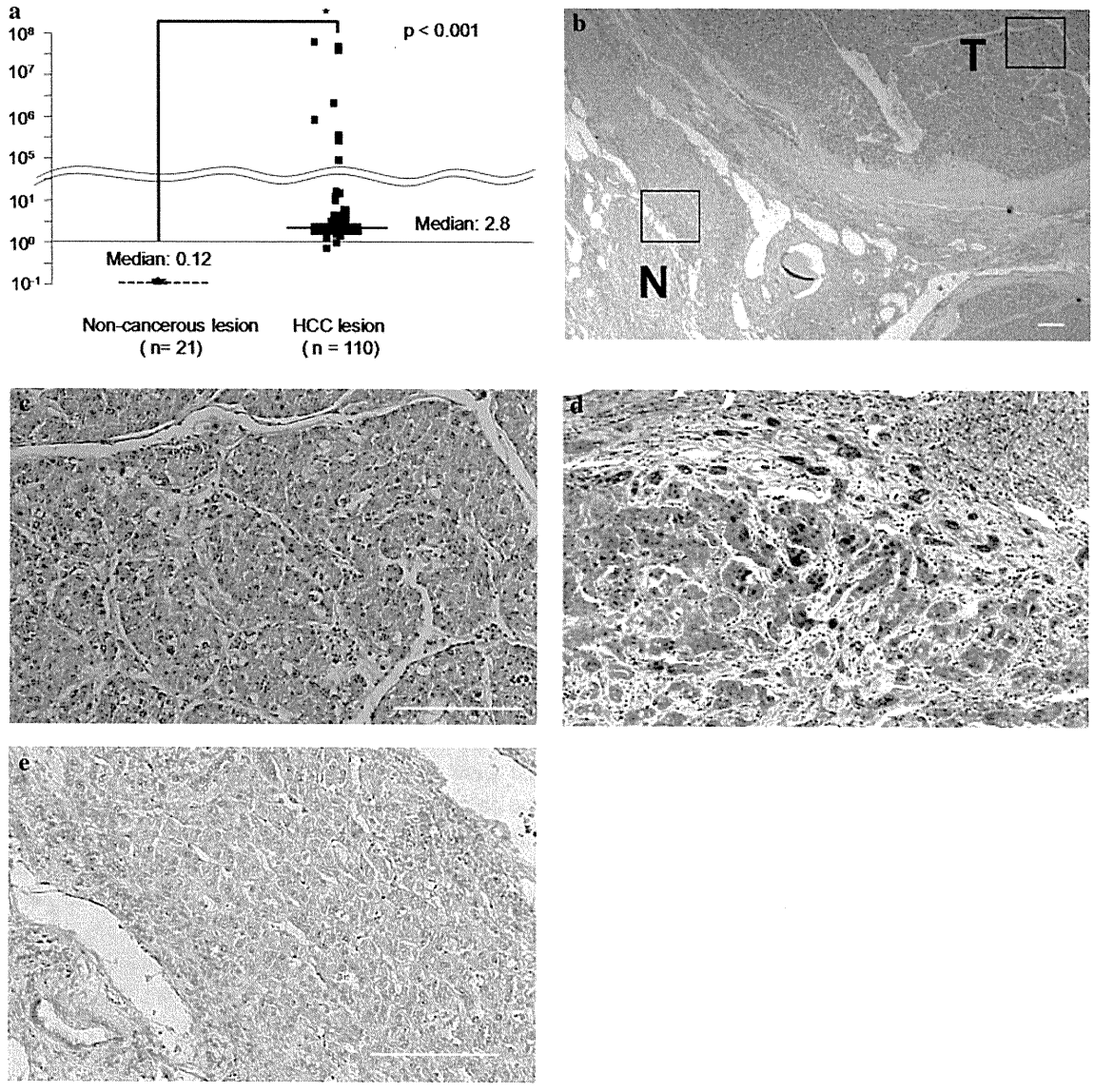

FIG. 1 JMJD1A mRNA and protein expression in resected HCC specimens. **a** JMJD1A mRNA expression determined by qRT-PCR. mRNA levels were normalized to endogenous β-actin mRNA (JMJD1A mRNA/β-actin mRNA) for expression in HCC tumors ($n = 110$) and noncancerous tissues ($n = 21$). Horizontal lines indicate median values for each group. **b–e** Representative immunohistochemical stains for JMJD1A: **b** HCC tissues (T) showed strong staining compared with corresponding noncancerous (N) tissues. **c**, **d** High-power fields showed that JMJD1A staining was localized in **c** the cytoplasm, and **d** both the nucleus and cytoplasm of HCC tissues. **e** JMJD1A was not detected in the corresponding noncancerous tissues. Scale bars 200 μm

tissues (Fig. 1b–d), but was not detected in corresponding noncancerous tissues (Fig. 1e). Of the 26 positively stained specimens, 22 showed staining only in the cytoplasm (Fig. 1c), and 4 showed staining in the nucleus and cytoplasm (Fig. 1d). In tissues positive for JMJD1A protein, the mRNA expression was higher than that observed in tissues negative for JMJD1A protein ($1.10 \pm 5.61 \times 10^7$ versus 2.97 ± 8.20, respectively; mean $\pm$ SD, $P < 0.0001$).

Based on the correlation between JMJD1A mRNA and protein expression, we grouped the specimens by high and low expression levels. To identify lesions with the highest positivity in both mRNA and protein, we used ROC curve analysis of protein reactivity to determine an appropriate cutoff value in the mRNA expression levels of corresponding samples (Supplementary Fig. 1). The area under the ROC curve was 0.893; the JMJD1A mRNA cutoff value of 2.15-fold gave sensitivity and specificity for positive JMJD1A protein reactivity of 84.6% and 80.3%, respectively. With this cutoff value, we divided HCC samples into JMJD1A-high ($n = 47$) and JMJD1A-low ($n = 63$) expression groups.

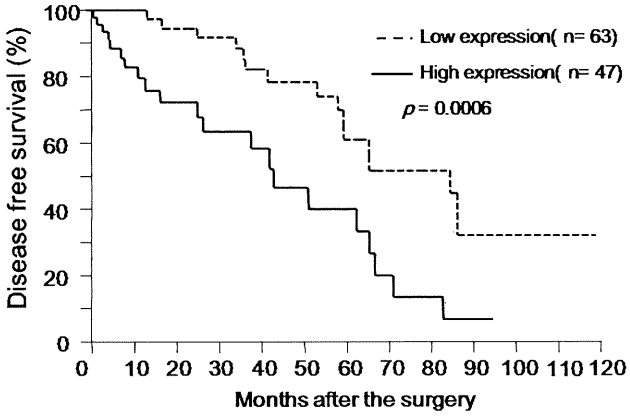

FIG. 2 Disease-free survival analysis according to protein and mRNA expression. Disease-free survival in patients with HCC after curative resection. Low and high JMJD1A expression was based on the cutoff value (2.15-fold) for mRNA expression

Patient Background and Survival in JMJD1A-High and JMJD1A-Low Groups

No significant differences were found in patient backgrounds in the JMJD1A-high and JMJD1A-low groups (Table 2). In addition, no significant differences were found in overall survival between groups ($P = 0.6477$; Table 3); the 3-year survival rates of JMJD1A-high and JMJD1A-low groups were 77.8% and 81.6%, respectively (data not shown). However, cancer-related disease-free survival was quite different between groups ($P = 0.0006$, Fig. 2); the 3-year survival rates of JMJD1A-high and JMJD1A-low groups were 63.5% and 88.5%, respectively ($P = 0.0006$; Table 3). Two clinicopathological parameters were also significantly associated with 3-year survival rates: Union for International Cancer Control (UICC) stage ($P = 0.0083$) and microscopic portal vein invasion (PVTT, $P = 0.0380$). However, multivariate Cox regression analysis of these parameters revealed that only JMJD1A expression remained an independent prognostic factor ($P = 0.0016$; hazard ratio = 3.00 [1.54–5.97], Table 3).

Effects of JMJD1A Expression on Growth, Invasion, and EMT in HCC Cells

To assess potential mechanisms of JMJD1A in HCC recurrence, an in vitro knockdown experiment was performed with siRNA in the HCC cell lines, HuH7, PLC, and HepG2. JMJD1A expression was lowest in PLC cells, but the differences among cell lines were not significant (Fig. 3a). Suppression of JMJD1A by siRNA was confirmed with qRT-PCR and Western blotting (Fig. 3b).

To evaluate the effects of hypoxia on HCC cells, we checked growth ability, invasion ability, and expression of EMT-related genes. As described previously, hypoxia reduced proliferation, increased invasive activity, and increased expression of EMT-related genes (Fig. 3c–e).[38,39]

Next, we evaluated the effect of suppressing JMJD1A in hypoxic and normoxic conditions.

After 72 h of treatment, hypoxia-induced growth inhibition was reduced with JMJD1A suppression (Fig. 3c); for example, in the HuH7 cell line, hypoxia inhibited proliferation by 15.5 ± 0.6% ($P = 0.047$); this was reduced to 2.4 ± 0.4% inhibition with hypoxia after JMJD1A siRNA treatment ($P < 0.01$). Similar effects were observed in the HepG2 and PLC cell lines (data not shown).

Additionally, in HuH7 cells, hypoxia stimulated invasion by 5.60 ± 0.1-fold ($P < 0.001$; Fig. 3d); however, this was reduced to only 2.93 ± 0.1-fold stimulation when JMJD1A was suppressed with siRNA treatment. Similar effects were observed in the other cell lines (data not shown). Therefore, siRNA treatment significantly reduced cell invasion stimulated by hypoxic conditions ($P < 0.01$).

EMT was evaluated by quantifying the expression of representative EMT-related mRNAs, including E-cadherin, N-cadherin, and Twist, by qRT-PCR (Fig. 3e). E-cadherin mRNA was expressed in all three cell lines, but N-cadherin and Twist mRNA were expressed at very low or undetectable levels. Hypoxic conditions caused a significant reduction in E-cadherin expression and overexpression of both N-cadherin and Twist in all cell lines. JMJD1A suppression with siRNA apparently reduced E-cadherin expression under normoxic conditions; however, under hypoxic conditions, JMJD1A suppression blocked the effects of hypoxia on E-cadherin, N-cadherin, and Twist mRNA expression.

DISCUSSION

In a preliminary study, we identified several molecular markers that could predict poor prognosis in patients with HCC.[40] Furthermore, we performed transcriptome analysis to explore new molecular indicators.[41–43] However, those insights were not directly related to hypoxia-inducible genes, which are thought to confer malignant potential in other cancers.

For this reason, we compared our previously identified hypoxia-inducible genes with microarray data derived from three HCC cell lines exposed to hypoxic conditions.[25] We found high mRNA levels for 26 genes (data not shown); of those, vascular epithelial growth factor ranked 3rd, egg-laying-defective nine homolog 3 ranked 5th, adrenomedullin ranked 21st, and JMJD1A ranked 9th. All had previously been reported to be poor prognostic factors for human malignancies.[25,44–46] Next, we performed a pilot study using previously published microarray data that represented 139 HCC samples (from patients not included

TABLE 2 Univariate analysis of patient characteristics and JMJD1A mRNA expression

Variable	JMJD1A mRNA expression		*P*-value
	Low ($n = 63$)	High ($n = 47$)	
Age (<65 years:65≤)	30:33	22:25	0.9329
Sex (male:female)	47:16	42:5	0.0844
HBV infection (negative:positive)	50:13	36:11	0.7284
HCV infection (negative:positive)	26:37	20:27	0.8926
Child–Pugh (A:B)	54:9	44:3	0.1766
AFP (<400 ng/ml:400≤)	50:13	33:14	0.2717
PIVKA-II (<40 mAU/m: 40≤)	59:4	45:2	0.6283
Preoperative TACE (yes:no)	35:28	28:19	0.6732
Tumor size (<3 cm:3≤)	19:44	13:34	0.7750
Tumor number (single:multiple)	22:41	16:31	0.9237
Macroscopic PVTT (absent:present)	53:10	32:15	0.0654
Macroscopic IM (absent:present)	43:20	31:16	0.7997
CLIP score (0 or 1:2<)	28:35	18:29	0.5174
JIS (0–2:3<)	46:17	31:16	0.4253
UICC stage (I or II:III or IV)	39:24	26:21	0.4874
Edmondson (I or II:III or IV)	31:32	21:26	0.6380
Microscopic PVTT (absent:present)	45:18	27:20	0.1279
Microscopic IM (absent:present)	50:13	34:13	0.3910
Background of the liver (NL or CH:LC)	37:26	26:21	0.7206

HBV hepatitis B virus, *HCV* hepatitis C virus, *AFP* α-fetoprotein, *PIVKA-II* protein induced by vitamin K absence or antagonist II, *TACE* transarterial chemoembolization, *PVTT* portal vein tumor thrombosis, *IM* intrahepatic metastasis, *CLIP* Cancer of the Liver Italian Program score, *JIS* Japan Integrated Staging, *UICC* Union for International Cancer Control, *NL* normal liver, *CH* chronic hepatitis, *LC* liver cirrhosis

TABLE 3 Univariate and multivariate analyses of disease-free survival

			Univariate	Multivariate	
	n	3-year DFS (%)	*P*-value	HR (95% CI)	*P*-value
Age (<65 years:65≤)	52:57	84.0:71.8	0.2010		
Sex (male:female)	89:21	75.8:86.2	0.6689		
HBV infection (negative:positive)	86:24	76.1:83.6	0.3393		
HCV infection (negative:positive)	46:64	83.2:74.6	0.0977		
Child–Pugh (A:B)	98:12	77.1:85.7	0.1716		
AFP (<400 ng/ml:400≤)	83:27	80.2:68.7	0.4958		
PIVKA-II (<40 mAU/ml:40≤)	104:6	77.5:100	0.4438		
Preoperative TACE (yes:no)	63:47	76.8:79.6	0.8302		
Tumor size (<3 cm:3≤)	32:78	83.4:75.9	0.1474		
Tumor number (single:multiple)	38:72	82.9:64.3	0.1273		
Macroscopic PVTT (absent:present)	85:25	80.8:67.5	0.1855		
Macroscopic IM (absent:present)	74:36	82.9:61.1	0.1167		
CLIP score (0 or 1:2<)	46:74	84.5:72.4	0.1418		
JIS (0–2:3<)	77:33	86.5:51.7	0.1045		
UICC stage (I or II:III or IV)	65:45	86.6:60.4	**0.0083**	2.1127 (0.967–4.098)	0.0517
Edmondson (I or II:III or IV)	52:58	82.6:74.1	0.8658		
Microscopic PVTT (absent:present)	72:38	86.4:47.9	**0.0380**	0.7813 (0.656–2.986)	0.3768
Microscopic IM (absent:present)	84:26	77.4:79.0	0.3984		
Background of the liver (NL or CH:LC)	63:47	78.5:76.9	0.7272		
JMJD1A (low:high)	63:47	88.5:63.5	**0.0006**	2.9984 (1.54–5.97)	**0.0016**

PVTT portal vein tumor thrombosis, *JIS* Japan Integrated Staging, *CLIP* Cancer of the Liver Italian Program score, *CH* chronic hepatitis, *LC* liver cirrhosis, *NL* normal liver, *DFS* disease-free survival

P-value < 0.05 was considered statistically significant, and *bold* indicates significant differences

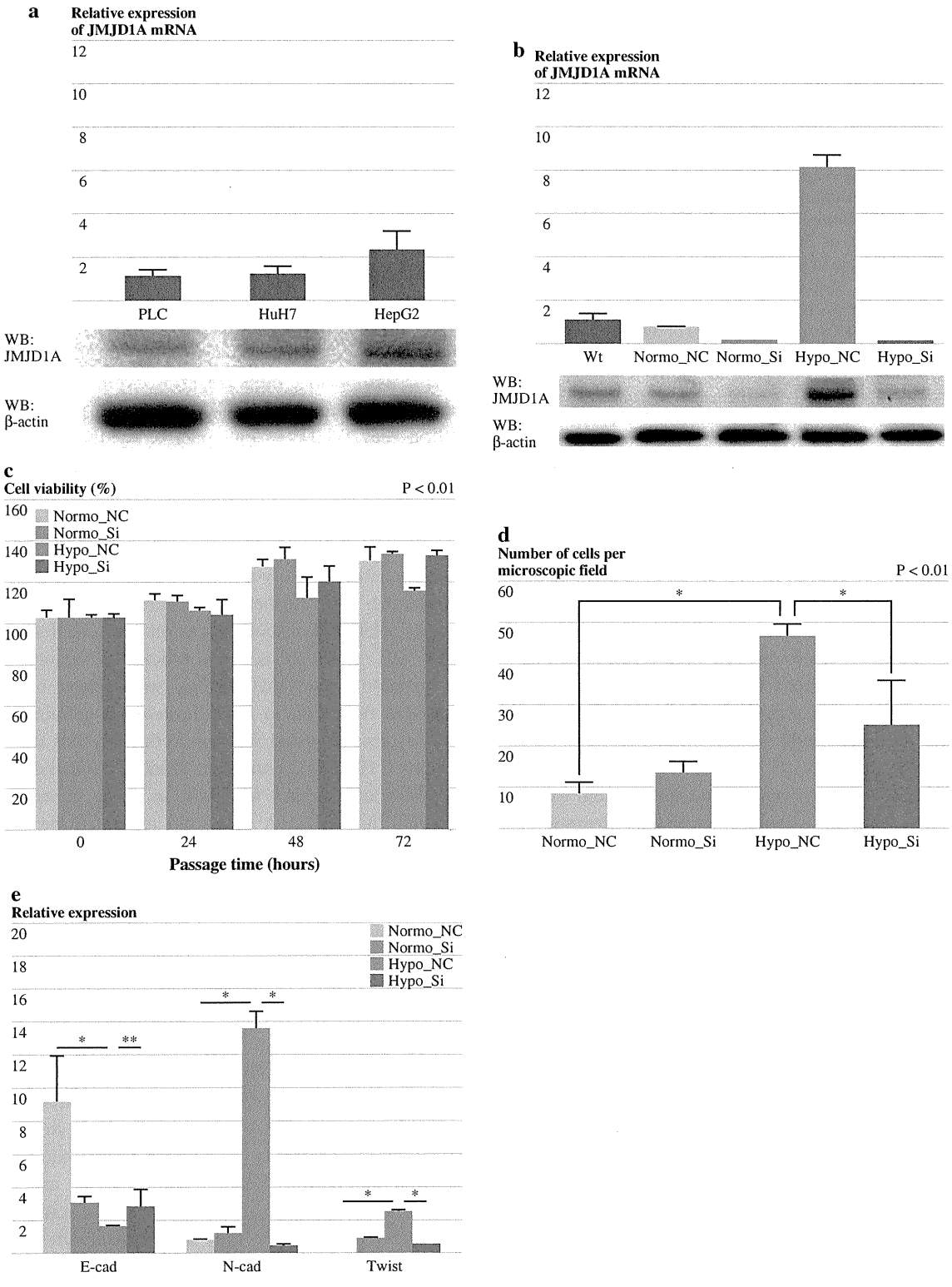

in the series reported herein).[43] We checked those four genes (vascular epithelial growth factor, egg-laying-defective nine homolog 3, adrenomedullin, and JMJD1A) to determine the relationship between expression level and prognosis using these microarray data; there, JMJD1A was the only significant prognostic marker for HCC ($P = 0.0234$, data not shown).

Based on the above preliminary data, in this study, we aimed to evaluate the role of JMJD1A expression in HCC. We demonstrated that JMJD1A expression was higher in

◀**FIG. 3** JMJD1A expression, proliferation, invasion, and EMT-related gene expression under hypoxic conditions. **a** JMJD1A mRNA (upper panel) and protein (lower panel) expression in HCC cell lines (PLC, HuH7, and HepG2). Normoxic conditions. The data represent mean ± SD. **b** PLC cells were treated with (Si) or without (NC) RNA interference of JMJD1A under hypoxic (hypo) or normoxic (normo) conditions. JMJD1A mRNA (upper panel) values represent mean ± SD; protein (lower panel) expression was normalized by endogenous β-actin expression. **c** Proliferation analysis (cell viability) of HuH7 cells under normoxia (normo) or hypoxia (hypo), with (Si) or without (NC) RNA interference of JMJD1A expression. The double, wavy line indicates a break in the numbering on the *Y*-axis. The data represent mean ± SD. *Significant difference between the values under the horizontal line. **d** Invasion assay shows the number of invasive HuH7 cells under normoxia (normo) or hypoxia (hypo), with (Si) or without (NC) RNA interference of JMJD1A expression. The data represent mean ± SD. *Significant difference between the values bracketed. **e** Epithelial–mesenchymal transition expression. Expression of representative mRNAs, E-cadherin (E-cad), N-cadherin (N-cad), and Twist was evaluated under normoxia (normo) or hypoxia (hypo), with (Si) or without (NC) RNA interference of JMJD1A expression. The data represent mean ± SD. Significant differences between values under the horizontal lines are indicated. (*$P < 0.01$, **$P = 0.0125$)

HCC tissues than in the corresponding background liver tissues. Furthermore, we found that high JMJD1A expression was a significant factor for predicting HCC recurrence. Finally, we showed that suppressing JMJD1A expression with siRNA treatment reduced the effects of hypoxia on malignant behaviors.

We demonstrated that both mRNA and protein expression were higher in HCC samples than in the corresponding normal liver tissues. Moreover, imuunostaining showed that JMJD1A was localized in both the nucleus and cytoplasm. This was unexpected, because JMJD1A is a histone H3 lysine 9 demethylase that activates transcription; therefore, JMJD1A would be expected to localize to the nucleus. However, according to Okada et al., when spermatids start to elongate, JMJD1A localizes to the cytoplasm and forms distinct foci; these foci persist until spermiogenesis and disappear in mature spermatozoa.[27] Therefore, in some settings, JMJD1A can localize to the cytoplasm. In this study, 26 of 87 specimens were immunohistochemically positive, including 22 samples that had stained only in the cytoplasm. Nevertheless, there was a significant correlation ($P < 0.0001$) between positive staining and JMJD1A mRNA expression. Thus, we concluded that the positive immunohistochemical reactivity represented true positive expression.

JMJD1A expression was significantly lower in noncancerous than in HCC samples. This suggested that JMJD1A was a potential marker for resected HCC. (Note that, because the JMJD1A-positive lesion might be variable in the tissue depending on relative hypoxia or other tumor-related reasons, this should be evaluated not in biopsy samples but in resected HCC samples.) Furthermore, hypoxia is thought to be induced by TACE in HCC tissue. Nonetheless, there was no significant change in JMJD1A expression with preoperative TACE. That suggested that JMJD1A expression was not only influenced by hypoxic conditions initiated by TACE. This is consistent with the fact that pulmonary metastasis after hepatic artery occlusion occurred only in some cases. In our hands, three HCC cell lines cultured under hypoxic conditions in vitro showed increases in JMJD1A mRNA expression that reached maximum levels (3- to 6-fold) after 48–72 h (data not shown).

Our finding that high JMJD1A expression was significantly associated with HCC recurrence gave rise to the notion that JMJD1A may play a significant role in the malignant transformation of HCC. Although JMJD1A was not significantly associated with overall survival, it was associated with disease-free survival. Several authors mentioned that the prognostic factors for survival after resection were not always coincident with those for HCC recurrence, and furthermore overall survival would be mainly related to vascular invasion and liver function.[47–49] Thus, our results are not in conflict with the consensus.

We also found that siRNA suppression of JMJD1A caused a reduction in hypoxia-induced cellular invasion. Our results suggested that this reduction was due to inhibition of EMT. Although no studies have indicated that JMJD1A could lead to EMT in other cancers, it was reported that JMJD1A positively regulated the expression of pluripotency-associated genes in embryonic stem cells, which self-renew indefinitely.[50,51] Moreover, in JMJD1A-deficient mice, mesenchymal tissues primarily developed into fat tissue in adults.[52] Taken together, the evidence suggests that JMJD1A may maintain the undifferentiated state, particularly in mesenchymal stem cells; thus, we hypothesized that, in epithelial cancer, such as HCC, JMJD1A expression may induce EMT. In the present study, our results on invasion and EMT expression were consistent with that hypothesis. Also, in proliferation assay, suppression of JMJD1A caused a decrease in the growth inhibition under hypoxic conditions. In hypoxic conditions, cells exhibit various behaviors to survive, and hypoxia-inducible genes play a critical role in eliciting cellular responses; for example, they may induce cell cycle arrest or apoptosis in irreversibly damaged cells.[53,54] Our data suggested that suppressing JMJD1A did not cause these cellular responses under hypoxic conditions.

In summary, our results suggest that JMJD1A is a sensitive recurrence marker, and JMJD1A can promote malignant transformation via EMT. Moreover, JMJD1A could be a promising therapeutic target for treating HCC.

CONFLICT OF INTEREST The authors declare no conflict of interest.

REFERENCES

1. Llovet JM, Burroughs A, Bruix J. Hepatocellular carcinoma. *Lancet.* 2003;362:1907–17.
2. Nagano H, Miyamoto A, Wada H, et al. Interferon-alpha and 5-fluorouracil combination therapy after palliative hepatic resection in patients with advanced hepatocellular carcinoma, portal venous tumor thrombus in the major trunk, and multiple nodules. *Cancer.* 2007;110:2493–501.
3. Nagano H. Treatment of advanced hepatocellular carcinoma: intraarterial infusion chemotherapy combined with interferon. *Oncology.* 2010;78 Suppl 1:142–7.
4. Murakami M, Nagano H, Kobayashi S, et al. The beneficial effect of preoperative transcatheter arterial chemoembolization for resectable hepatocellular carcinoma: Implication of circulating cancer cells detecting alpha-fetoprotein mRNA. *Mol Therapeut Med.* 2010;1:485–91.
5. Llovet JM, Bruix J. Molecular targeted therapies in hepatocellular carcinoma. *Hepatology.* 2008;48:1312–27.
6. Liou TC, Shih SC, Kao CR, Chou SY, Lin SC, Wang HY. Pulmonary metastasis of hepatocellular carcinoma associated with transarterial chemoembolization. *J Hepatol.* 1995;23:563–8.
7. Song BC, Chung YH, Kim JA, et al. Association between insulin-like growth factor-2 and metastases after transcatheter arterial chemoembolization in patients with hepatocellular carcinoma: a prospective study. *Cancer.* 2001;91:2386–93.
8. Ebos JM, Lee CR, Cruz-Munoz W, Bjarnason GA, Christensen JG, Kerbel RS. Accelerated metastasis after short-term treatment with a potent inhibitor of tumor angiogenesis. *Cancer Cell.* 2009;15:232–9.
9. Paez-Ribes M, Allen E, Hudock J, et al. Antiangiogenic therapy elicits malignant progression of tumors to increased local invasion and distant metastasis. *Cancer Cell.* 2009;15:220–31.
10. Semenza GL. Hypoxia and cancer. *Cancer Metastasis Rev.* 2007;26:223–4.
11. Colpaert C, Vermeulen P, van Beest P, et al. Intratumoral hypoxia resulting in the presence of a fibrotic focus is an independent predictor of early distant relapse in lymph node-negative breast cancer patients. *Histopathology.* 2001;39:416–25.
12. Koukourakis MI, Giatromanolaki A, Sivridis E, et al. Hypoxia-regulated carbonic anhydrase-9 (CA9) relates to poor vascularization and resistance of squamous cell head and neck cancer to chemoradiotherapy. *Clin Cancer Res.* 2001;7:3399–403.
13. Giatromanolaki A, Koukourakis MI, Sivridis E, et al. Expression of hypoxia-inducible carbonic anhydrase-9 relates to angiogenic pathways and independently to poor outcome in non-small cell lung cancer. *Cancer Res.* 2001;61:7992–8.
14. Fyles A, Milosevic M, Hedley D, et al. Tumor hypoxia has independent predictor impact only in patients with node-negative cervix cancer. *J Clin Oncol.* 2002;20:680–7.
15. Vaupel P, Mayer A. Hypoxia in cancer: significance and impact on clinical outcome. *Cancer Metastasis Rev.* 2007;26:225–39.
16. Wada H, Nagano H, Yamamoto H, et al. Expression pattern of angiogenic factors and prognosis after hepatic resection in hepatocellular carcinoma: importance of angiopoietin-2 and hypoxia-induced factor-1 alpha. *Liver Int.* 2006;26:414–23.
17. Graeber TG, Osmanian C, Jacks T, et al. Hypoxia-mediated selection of cells with diminished apoptotic potential in solid tumours. *Nature.* 1996;379:88–91.
18. Gupta S, Kobayashi S, Phongkitkarun S, Broemeling LD, Kan Z. Effect of transcatheter hepatic arterial embolization on angiogenesis in an animal model. *Invest Radiol.* 2006;41:516–21.
19. Li X, Feng GS, Zheng CS, Zhuo CK, Liu X. Influence of transarterial chemoembolization on angiogenesis and expression of vascular endothelial growth factor and basic fibroblast growth factor in rat with Walker-256 transplanted hepatoma: an experimental study. *World J Gastroenterol.* 2003;9:2445–9.
20. Liao XF, Yi JL, Li XR, Deng W, Yang ZF, Tian G. Angiogenesis in rabbit hepatic tumor after transcatheter arterial embolization. *World J Gastroenterol.* 2004;10:1885–9.
21. Forsythe JA, Jiang BH, Iyer NV, et al. Activation of vascular endothelial growth factor gene transcription by hypoxia-inducible factor 1. *Mol Cell Biol.* 1996;16:4604–13.
22. Chi JT, Wang Z, Nuyten DS, et al. Gene expression programs in response to hypoxia: cell type specificity and prognostic significance in human cancers. *PLoS Med.* 2006;3:e47.
23. Brahimi-Horn MC, Chiche J, Pouyssegur J. Hypoxia and cancer. *J Mol Med.* 2007;85:1301–7.
24. van Malenstein H, Gevaert O, Libbrecht L, et al. A seven-gene set associated with chronic hypoxia of prognostic importance in hepatocellular carcinoma. *Clin Cancer Res.* 2010;16:4278–88.
25. Uemura M, Yamamoto H, Takemasa I, et al. JMJD1A is a novel prognostic marker for colorectal cancer; Identification from in vivo hypoxic tumor cells. *Clin Cancer Res.* 2010;18:4636–46.
26. Arun C, London NJ, Hemingway DM. Prognostic significance of elevated endothelin-1 levels in patients with colorectal cancer. *Int J Biol Markers.* 2004;19:32–7.
27. Okada Y, Scott G, Ray MK, Mishina Y, Zhang Y. Histone demethylase JHDM2A is critical for Tnp1 and Prm1 transcription and spermatogenesis. *Nature.* 2007;450:119–23.
28. Yamane K, Toumazou C, Tsukada Y, et al. JHDM2A, a JmjC-containing H3K9 demethylase, facilitates transcription activation by androgen receptor. *Cell.* 2006;125:483–95.
29. Adam K, Erinn R, Denise C, Olga R, Sully F, Amato G. Regulation of the histone demethylase JMJD1A by hypoxia-inducible factor 1 enhances hypoxic gene expression and tumor growth. *Mol Cell Biol.* 2010;30:344–53.
30. Hayashi N, Yamamoto H, Hiraoka N, et al. Differential expression of cyclooxygenase-2 (COX-2) in human bile duct epithelial cells and bile duct neoplasm. *Hepatology.* 2001;34:638–50.
31. Yamamoto H, Kondo M, Nakamori S, et al. JTE-522, a cyclooxygenase-2 inhibitor, is an effective chemopreventive agent against rat experimental liver fibrosis1. *Gastroenterology.* 2003;125:556–71.
32. Yang MH, Chen CL, Chau GY, et al. Comprehensive analysis of the independent effect of twist and snail in promoting metastasis of hepatocellular carcinoma. *Hepatology.* 2009;50:1464–74.
33. Ning B, Ding J, Yin C, et al. Hepatocyte nuclear factor 4 alpha suppresses the development of hepatocellular carcinoma. *Cancer Res.* 2010;70:7640–51.
34. Ding ZB, Shi YH, Zhou J, et al. Liver-intestine cadherin predicts microvascular invasion and poor prognosis of hepatitis B virus-positive hepatocellular carcinoma. *Cancer.* 2009;115:4753–65.
35. Shiokawa T, Hattori Y, Kawano K, et al. Effect of polyethylene glycol linker chain length of folate-linked microemulsions loading aclacinomycin A on targeting ability and antitumor effect in vitro and in vivo. *Clin Cancer Res.* 2005;11:2018–25.
36. Seton-Rogers SE, Lu Y, Hines LM, et al. Cooperation of the ErbB2 receptor and transforming growth factor beta in induction of migration and invasion in mammary epithelial cells. *Proc Natl Acad Sci U S A.* 2004;101:1257–62.
37. Youden WJ. Index for rating diagnostic tests. *Cancer.* 1950;3:32–5.
38. Yang MH, Wu MZ, Chiou SH, et al. Direct regulation of TWIST by HIF-1alpha promotes metastasis. *Nat Cell Biol.* 2008;10:295–305.
39. Liu L, Ren ZG, Shen Y, et al. Influence of hepatic artery occlusion on tumor growth and metastatic potential in a human

orthotopic hepatoma nude mouse model: relevance of epithelial-mesenchymal transition. *Cancer Sci.* 2009;101:120–8.
40. Damdinsuren B, Nagano H, Kondo M, et al. TGF-beta1-induced cell growth arrest and partial differentiation is related to the suppression of Id1 in human hepatoma cells. *Oncol Rep.* 2006;15:401–8.
41. Kittaka N, Takemasa I, Seno S, et al. Exploration of potential genomic portraits associated with intrahepatic recurrence in human hepatocellular carcinoma. *Ann Surg Oncol.* 2010;17:3145–54.
42. Kurokawa Y, Honma K, Takemasa I, et al. Central genetic alterations common to all HCV-positive, HBV-positive and non-B, non-C hepatocellular carcinoma: a new approach to identify novel tumor markers. *Int J Oncol.* 2006;28:383–91.
43. Yoshioka S, Takemasa I, Nagano H, et al. Molecular prediction of early recurrence after resection of hepatocellular carcinoma. *Eur J Cancer.* 2009;45:881–9.
44. Ishigami SI, Arii S, Furutani M, et al. Predictive value of vascular endothelial growth factor (VEGF) in metastasis and prognosis of human colorectal cancer. *Br J Cancer.* 1998;78:1379–84.
45. Couvelard A, Deschamps L, Rebours V, et al. Overexpression of the oxygen sensors PHD-1, PHD-2, PHD-3, and FIH Is associated with tumor aggressiveness in pancreatic endocrine tumors. *Clin Cancer Res.* 2008;14:6634–9.
46. Hata K, Takebayashi Y, Akiba S, et al. Expression of the adrenomedullin gene in epithelial ovarian cancer. *Mol Hum Reprod.* 2000;6:867–72.
47. Poon RT, Ng IO, Fan ST, et al. Clinicopathologic features of long-term survivors and disease-free survivors after resection of hepatocellular carcinoma: a study of a prospective cohort. *J Clin Oncol.* 2001;19:3037–44.
48. Arii S, Tanaka J, Yamazoe Y, et al. Predictive factors for intrahepatic recurrence of hepatocellular carcinoma after partial hepatectomy. *Cancer.* 1992:69:913–9.
49. The Japan Society of Hepatology. Clinical Practice Guidelines for Hepatocellular Carcinoma - The Japan Society of Hepatology 2009 update. *Hepatol Res.* 2010;40:2–144.
50. McGraw S, Vigneault C, Sirard MA. Temporal expression of factors involved in chromatin remodeling and in gene regulation during early bovine in vitro embryo development. *Reproduction.* 2007;133:597–608.
51. Loh YH, Zhang W, Chen X, George J, Ng HH. Jmjd1a and Jmjd2c histone H3 Lys 9 demethylases regulate self-renewal in embryonic stem cells. *Genes Dev.* 2007;21:2545–57.
52. Inagaki T, Tachibana M, Magoori K, et al. Obesity and metabolic syndrome in histone demethylase JHDM2a-deficient mice. *Genes Cells.* 2009;14:991–1001.
53. Semenza GL. Targeting HIF-1 for cancer therapy. *Nat Rev Cancer.* 2003;3:721–32.
54. Simon MC, Keith B. The role of oxygen availability in embryonic development and stem cell function. *Nat Rev Mol Cell Biol.* 2008;9:285–96.

OPEN ACCESS Freely available online

PLoS one

MicroRNA Profile Predicts Recurrence after Resection in Patients with Hepatocellular Carcinoma within the Milan Criteria

Fumiaki Sato[1]*, Etsuro Hatano[2], Koji Kitamura[2], Akira Myomoto[3,4], Takeshi Fujiwara[1], Satoko Takizawa[3], Soken Tsuchiya[1], Gozoh Tsujimoto[4], Shinji Uemoto[2], Kazuharu Shimizu[1]

1 Department of Nanobio Drug Discovery, Graduate School of Pharmaceutical Sciences, Kyoto University, Kyoto, Japan, **2** Department of Surgery, Graduate School of Medicine, Kyoto University, Kyoto, Japan, **3** New Frontiers Research Laboratories, Toray Industries, Inc. Kanagawa, Japan, **4** Department of Pharmacogenomics, Graduate School of Pharmaceutical Sciences, Kyoto University, Kyoto, Japan

Abstract

Objective: Hepatocellular carcinoma (HCC) is difficult to manage due to the high frequency of post-surgical recurrence. Early detection of the HCC recurrence after liver resection is important in making further therapeutic options, such as salvage liver transplantation. In this study, we utilized microRNA expression profiling to assess the risk of HCC recurrence after liver resection.

Methods: We examined microRNA expression profiling in paired tumor and non-tumor liver tissues from 73 HCC patients who satisfied the Milan Criteria. We constructed prediction models of recurrence-free survival using the Cox proportional hazard model and principal component analysis. The prediction efficiency was assessed by the leave-one-out cross-validation method, and the time-averaged area under the ROC curve (ta-AUROC).

Results: The univariate Cox analysis identified 13 and 56 recurrence-related microRNAs in the tumor and non-tumor tissues, such as miR-96. The number of recurrence-related microRNAs was significantly larger in the non-tumor-derived microRNAs (N-miRs) than in the tumor-derived microRNAs (T-miRs, $P<0.0001$). The best ta-AUROC using the whole dataset, T-miRs, N-miRs, and clinicopathological dataset were 0.8281, 0.7530, 0.7152, and 0.6835, respectively. The recurrence-free survival curve of the low-risk group stratified by the best model was significantly better than that of the high-risk group (Log-rank: $P=0.00029$). The T-miRs tend to predict early recurrence better than late recurrence, whereas N-miRs tend to predict late recurrence better ($P<0.0001$). This finding supports the concept of early recurrence by the dissemination of primary tumor cells and multicentric late recurrence by the 'field effect'.

Conclusion: microRNA profiling can predict HCC recurrence in Milan criteria cases.

Citation: Sato F, Hatano E, Kitamura K, Myomoto A, Fujiwara T, et al. (2011) MicroRNA Profile Predicts Recurrence after Resection in Patients with Hepatocellular Carcinoma within the Milan Criteria. PLoS ONE 6(1): e16435. doi:10.1371/journal.pone.0016435

Editor: Hang Nguyen, Emory University, United States of America

Received September 3, 2010; **Accepted** December 24, 2010; **Published** January 27, 2011

Funding: This work was supported by a Japanese federal fund promoting academia-industry collaboration, "Grant for Practical Application of University R&D Results under the Matching Fund Method, from a Japanese federal organization, the New Energy and Industrial Technology Development Organization (NEDO), Japan". The funders had no role in study design, data collection and analysis, decision to publish, or preparation of the manuscript. Toray Industries, Inc. is a funder due to employment of Arira Myomoto and Satoko Takizawa, who provided technical support to conduct this project, but did not have a role in study design, data collection and analysis, decision to publish, or preparation of the manuscript.

Competing Interests: Fumiaki Sato, Etsuro Hatano, Akira Myomoto, Satoko Takizawa, and Kazuharu Shimizu are involved in a collaborative contract between Kyoto University and Toray Industries, Inc. under the regulation of "Grant for Practical Application of University R&D Results under the Matching Fund Method, from the NEDO". Akira Myomoto and Satoko Takizawa are employees of Toray Industries, Inc. In this study, the authors use the product of Toray Industries, Inc., which is a substrate of DNA microarray, "3D-Gene™". There is no other conflict of interest. This does not alter the authors' adherence to all the PLoS ONE policies on sharing data and materials.

* E-mail: fsato@pharm.kyoto-u.ac.jp

Introduction

Hepatocellular carcinoma (HCC) is one of the most common malignancies worldwide, and is the fourth most common cause of mortality [1,2]. In addition, its incidence is increasing in many countries [3,4]. HCC is difficult to manage, as compared with other common malignant diseases due to the high percentage of co-existing liver cirrhosis. The impaired liver function caused by liver cirrhosis often restricts treatment options, even for early HCC. Liver resection (LR) and orthotopic liver transplantation (OLT) are considered as the only two potentially curative treatment options for HCC. Currently, the Milan Criteria (i.e., solitary tumor $\leqq$5 cm, or 2 or 3 tumors $\leqq$3 cm) [5] are widely accepted as the selection Criteria for OLT in HCC patients. For HCC patients with severe liver cirrhosis (Child-Pugh C), OLT is considered the first-line treatment. In these cases, LR is contraindicated because of impaired liver function. In contrast, there has been an intense debate about which treatment option of LR or OLT is the optimal initial treatment for HCC patients with no to mild liver cirrhosis (Child-Pugh A/B). Some authors have

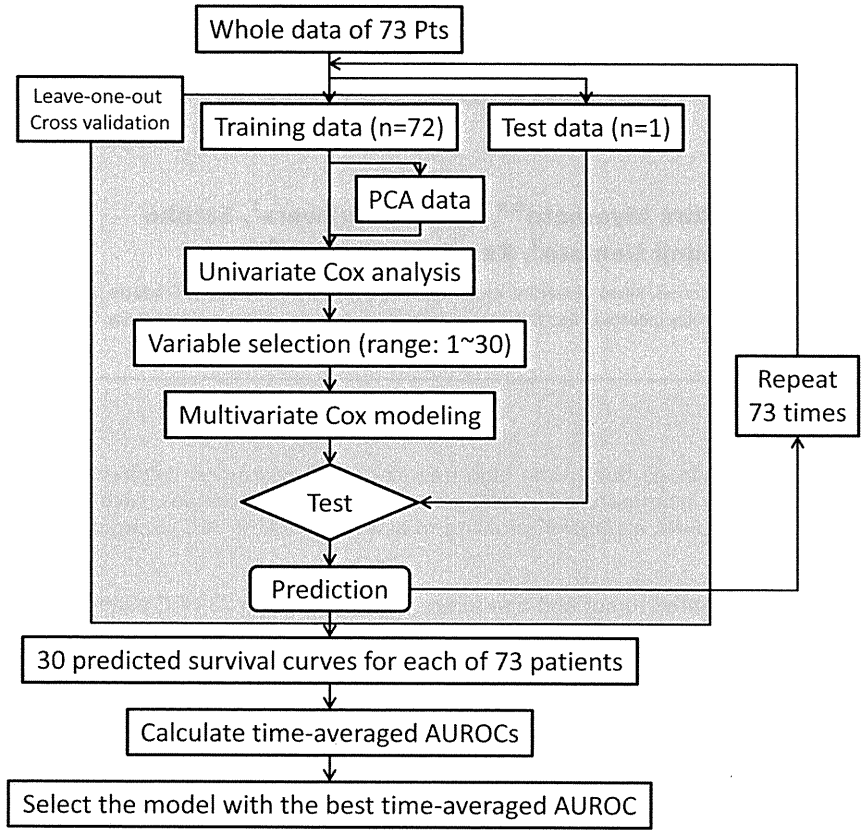

Figure 1. Flow chart of the prediction model construction and validation. To establish prediction models, the leave-one-out cross-validation method (LOOCV), principal component analysis (PCA), and Cox proportional hazard (CoxPH) models were used. In each LOOCV cycle, the variables of the training datasets or principal component (PC) dataset were prioritized by univariate CoxPH model analysis. Next, multivariate CoxPH models were developed using 1~30 top-ranked variables, and 30 predicted recurrence-free survival curves were the output for a test dataset. After 73 LOOCV cycles, 73×30 predicted recurrence-free survival curves were generated. For each number of variables used, the time-averaged AUROC was calculated using a set of 73 predicted survival curves. Finally, a model with the best time-averaged AUROC was selected.
doi:10.1371/journal.pone.0016435.g001

recommended OLT as the first-line treatment for HCC fulfilling the Milan Criteria given the lower tumor recurrence rate after OLT[6,7]. On the other hand, due to the shortage of donor organs, many liver transplant centers choose LR for HCC patients with Child-Pugh A/B, and who satisfy the Milan Criteria. Therefore, the strategy of a primary LR and salvage transplantation for intrahepatic HCC recurrence is a reasonable tactic for early resectable HCC with preserved liver function. In this strategy, it is important to predict recurrent tumors for selecting the follow-up protocol of patients after LR.

In our previous reports, we screened prognostic factors from various clinical features, and found that co-existing cirrhosis correlated with the outcomes of HCC cases within the Milan Criteria[8]. Moreover, utilizing clinical factors, we also determined a safe expanded selection criteria for the indications of living donor liver transplantation in HCC patients beyond the Milan Criteria[9]. To obtain better-optimized stratification criteria and a more accurate prediction of recurrence, biological information and biomarkers derived from "OMICS" approaches, e.g., transcriptomics and proteomics, will be powerful tools.

MicroRNAs are a class of small non-coding RNAs [19–23 nucleotides (nt)] that have been found in animal and plant cells. As of today, 1049 human microRNAs are registered in the miRBase database (Release 16, September, 2010)[10–13]. MicroRNA genes are transcribed as non-coding transcripts, and are processed through a series of sequential steps involving the RNase III enzymes, Drosha and Dicer. The processed microRNAs are finally incorporated into the RNA-induced silencing complex (RISC) to mediate the target mRNA repression of translation and/or degradation. It has been reported that microRNAs are involved in physiological and pathological functions, such as the regulation of developmental timing and pattern formation[14], the restriction of differentiation potential[15], chromatin rearrangements[16], and carcinogenesis[17]. Many of the mechanistic details still remain unknown.

In the last decade, gene expression profiling has been utilized to classify the type of HCC and to predict the recurrence and survival of HCC patients [18–21]. Moreover, recent microarray technology has been utilized to analyze a comprehensive microRNA expression profiling of HCC [22,23]. However, a microarray-based prediction of HCC recurrence, especially for early HCC patients, have not been reported.

Previously, we developed a highly sensitive platforms for both mRNA and microRNA expression profiling [24]. Our ultimate goal is to apply microarray technology into the clinical field. Thus, we previously evaluated a microRNA-microarray platform as a future IVDMIA (*in vitro* diagnostic multivariate index assay) device using analytical procedures recommended by the Microarray quality control (MAQC) project [25]. In this study, we examined whether microRNA microarray technology can predict recurrent HCC after LR for patients who satisfying the Milan Criteria.

Table 1. Clinical Features of 73 HCC patients within Milan Criteria and Univariate Cox Proportional Hazard Model.

			Cox proportional hazard model	
Clinical features			**hazard ratio**	**p-value**
Age	mean, range			
		65.8 (40–88)	0.981	0.228
Gender				
	female	19	1.077	0.825
	male	54		
Tumor size (Max diameter)	mean±SD			
		3.2±1.0	0.833	0.235
Child-Pugh classification				
	A	69	1.924	0.277
	B	4		
Cirrhosis				
	(-)	36	1.246	0.463
	(+)	37		
Tumor Grade				
	well	21	0.982	0.938
	moderate	45		
	poor	7		
T factor				
	T1	7	1.692	0.0131
	T2	51		
	T3	13		
	T4	2		
HBV antigen				
	(-)	61	2.033	0.0490
	(+)	12		
HCV antibody				
	(-)	22	1.119	0.734
	(+)	51		

Tumor Grade and Tumor factor are recorded according to the General Rules for the Clinical and Pathological Study of Primary Liver Cancer (26).

doi:10.1371/journal.pone.0016435.t001

Materials and Methods

Patients

Between January, 1997 and March, 2007, 639 patients with HCC underwent hepatic resection as a primary curative treatment. Among these patients, 73 patients satisfied the following patient enrollment criteria; 1) no preoperative therapy, 2) within the Milan Criteria, 3) with Child-Pugh A-B level cirrhosis, 4) no or minimum vessel invasion (pathological Vp0-2 and Vv0-1 according to the General Rules for the Clinical and Pathological Study of Primary Liver Cancer, the 4th edition [26]), 5) availability of frozen paired tumor and non-tumor liver tissues, and 6) the quality of extracted RNA was good enough for microarray analysis. This study was approved by the Institutional Review Board of School of Medicine and Kyoto University Hospital, and the Human Tissue Samples Ethics Committee for R&D, Toray Ind., Inc. All patients gave their written informed consent to the sample collection and analyses described in the present study, in agreement with the Declaration of Helsinki.

RNA extraction

Tumor and non-tumor tissues were obtained and frozen in liquid nitrogen immediately after hepatic resection, and were stored in liquid nitrogen until RNA extraction. The total RNA samples were extracted by a phenol-chloroform RNA extraction method (Trizol; Invitrogen, Carlsbad, Calif., USA). The quality of the purified total RNAs was analyzed by a Bioanalyzer 2100 (Agilent Technologies, Palo Alto, Calif., USA). The criteria for the use of a sample was that the 18s and 28s ribosomal RNA peaks were twice or more higher than the other peaks, as previously described [27]. The RNA Integrity Numbers (RIN) of Bioanalyzer software for all samples was more than 5.

MicroRNA expression profiling

We utilized Toray's 3D-Gene^{TM} human microRNA chips (miRBase version 12) for microRNA expression profiling. The reproducibility and comparability to Taqman RT-PCR, and the experimental procedures of Toray's microarray, were described previously [25]. Briefly, for each patient, 500 ng of total RNA derived from both tumor and non-tumor samples were labeled using miRCURY LNA^{TM} microRNA Power Labeling Kits Hy5 (Exiqon, Vedbaek, Denmark). The labeled samples were individually hybridized onto the DNA chip surface, and were incubated at 42°C for 16 hours. The washed and dried DNA chip in an ozone-free environment was scanned using a ProScanArray^{TM} microarray scanner (PerkinElmer Inc. Waltham, MA). The obtained microarray images were analyzed using Genepix Pro^{TM} 4.0 software (Molecular Device, Sunnyvale, CA). In this study, the median values of the foreground signal minus the local background were represented as the feature intensities. The microRNA expression profile of all samples was illustrated as a heatmap in Figure S1.

Data analyses procedures

In this study, the recurrence-free survival was defined as the time between the operation date and the date when the recurrent tumor/tumors were identified. The clinical dataset consists of 63 clinicopathological information points (Table S1). All data obtained from the microarray experiments were normalized by a quantile normalization method [28], and then were filtered (75 percentile of miR expression >6 in log2 scale). Thus, 193 microRNAs were selected, and finally 579 data points (579 = 193×3, T-miR, N-miR, and T/N ratio) for each patient were used for further prediction model construction. The model construction procedure is illustrated in a flow chart (Figure 1). All statistical analyses and prediction model construction were performed using Matlab 2010a software (Mathworks, Natick, MA, USA). The detailed data process procedures are described in a supplemental file. In this study, p-values less than 0.05 were considered as statistically significant. All microRNA microarray data were registered into NCBI's Gene Expression Omnibus (GEO) database (http://www.ncbi.nlm.nih.gov/projects/geo/). The accession numbers are GSE21362 for series IDs, and GSM533698~533843 for sample IDs.

Results

Patients' characteristics

Table 1 summarizes the clinicopathological characteristics of the patients. All patients were treated with curative surgical liver resection. The mean recurrence-free survival of the complete cases (n = 45) was 618 days (standard deviation: 517 days). The mean follow-up periods of the censored cases (n = 28) was 1902 days.

Table 2. Recurrence-related microRNAs.

Recurrence-related microRNAs in tumor tissues						Recurrence-related microRNAs in non-tumor tissues (Top 20 out of 56 significant miRs)					
Rank	**microRNA**	**hazard ratio**	**miR-type**	**p-value**	**FDR**	**Rank**	**microRNA**	**hazard ratio**	**miR-type**	**p-value**	**FDR**
1	miR-100	0.5170	Ts-miR	<0.0001	0.011	1	miR-27a	7.4696	OncomiR	<0.0001	0.004
2	miR-99a	0.6318	Ts-miR	0.0006	0.035	2	miR-24	11.5691	OncomiR	0.0001	0.004
3	miR-99b	0.6087	Ts-miR	0.0013	0.040	3	miR-96	1.4868	OncomiR	0.0002	0.003
4	miR-125b	0.8062	Ts-miR	0.0028	0.048	4	miR-21	1.6847	OncomiR	0.0004	0.006
5	miR-378	0.6339	Ts-miR	0.0043	0.055	5	miR-18a	1.9046	OncomiR	0.0007	0.007
6	miR-129-5p	0.6888	Ts-miR	0.0075	0.083	6	miR-23a	5.5879	OncomiR	0.0010	0.007
7	miR-125a-5p	0.7441	Ts-miR	0.0089	0.080	7	miR-18b	1.6114	OncomiR	0.0013	0.007
8	miR-497	0.7737	Ts-miR	0.0123	0.090	8	miR-142-3p	1.4802	OncomiR	0.0018	0.007
9	miR-22	0.5470	Ts-miR	0.0141	0.085	9	miR-362-3p	1.4718	OncomiR	0.0020	0.006
10	miR-140-3p	0.5603	Ts-miR	0.0306	0.208	10	miR-1202	0.7592	Ts-miR	0.0021	0.006
11	miR-145	0.7531	Ts-miR	0.0341	0.213	11	let-7e	3.3158	OncomiR	0.0025	0.004
12	miR-221	1.4608	OncomiR	0.0441	0.266	12	let-7f	5.6499	OncomiR	0.0039	0.009
13	miR-195	0.7803	Ts-miR	0.0487	0.262	13	miR-191	7.4922	OncomiR	0.0047	0.011
						14	miR-107	6.0708	OncomiR	0.0057	0.014
						15	miR-148a	0.5922	Ts-miR	0.0061	0.013
						16	miR-222	1.5374	OncomiR	0.0077	0.013
						17	miR-103	5.5941	OncomiR	0.0086	0.012
						18	miR-126*	2.2102	OncomiR	0.0087	0.012
						19	miR-425	2.1610	OncomiR	0.0089	0.012
						20	miR-378	0.6406	Ts-miR	0.0090	0.011

This table lists hazard ratio and p-value calculated by an univariate Cox's propotional hazard model for each microRNA. MicroRNAs which hazard ratio is greater than 1 were correlated with frequent recurrence, and are potential **oncomiRs**. In contrast, microRNAs with hazard ratio less than 1 were associated with good recurrence-free survivals, and would be a tumor-suppressor miRs (**Ts-miR**). The number (=56) of recurrence-related microRNAs in non-tumor tissues is significantly larger than that (=13) in tumor tissues (Fisher's exact t-test: $p<0.00001$). False discovery rate (FDR) were estimated by permutation analysis.

doi:10.1371/journal.pone.0016435.t002

Among the 73 patients, 45 had recurrent tumors. The types of initial recurrences were intrahepatic, extrahepatic, and both for 41, 2, and 2 patients, respectively. According to univariate Cox proportional hazard model (CoxPH) analysis, T-factor and HBV infection are significantly associated with a shorter recurrent-free survival ($P=0.0131$ and 0.0490, respectively).

Recurrence-related microRNA signature

As the first step in this analysis, we utilized univariate CoxPH to identify recurrence-related microRNAs (Table 2). Interestingly, most of the identified tumor-derived microRNAs (T-miRs) were negatively associated with HCC recurrence, which suggests that tumor-suppressor microRNAs are down-regulated in tumor tissues. On the other hand, most of the identified non-tumor-derived microRNAs (N-miRs), which are ranked in the top-20, were positively associated with HCC recurrence, which indicated that oncogenic microRNAs are predominantly up-regulated in non-tumor tissues. In addition, the number of miRs significantly correlated with HCC recurrence was larger in non-tumor tissues than in tumor tissues (Fisher's exact test: $p<0.0001$). As the second step, we applied principal component analysis (PCA) to the univariate CoxPH analysis. The five principal components (PCs) of the microRNA expression profile were significantly correlated to the recurrence-free survival of HCC (Table 3). To show the clinical significance of each PC, the correlated clinical features of each PC are also listed in Table 3. For example, PC3 is a HBV and AFP related PC, and PC16 is a T-factor related one. A 3-dimentional scatter plot shows that the top 3 ranked PCs correlated to the recurrence-free survival of HCC patients (Figure 2).

Constructing prediction models of HCC recurrence-free survival

The prediction model was constructed by multivariate CoxPH models with leave-one-out cross-validation method (Figure 1). The accuracy of each prediction was evaluated by a time-averaged AUROC ($\overline{\text{AUROC}}$) between 6 months and 5 years. The $\overline{\text{AUROC}}$ changes depending upon the sample tissues, inclusion or exclusion of PCA, the number of variables used for constructing prediction models. Among the various conditions, the best $\overline{\text{AUROC}}$ (=0.8281) was achieved when the model was constructed using top-12 PCs data generated from an integrated dataset consisting of T-miRs and N-miRs, and T/N ratios (Figure 3). Figure 4 shows the change of AUROCs for different time points between 6 months and 5 years after LR. This model can predict early recurrences better (the best AUROC = 0.9276 at 1 year after LR) than late recurrences. Next, according to this prediction model, the 73 cases were stratified into Low- (n = 37) and High-risk (n = 36) groups. Consequently, the Kaplan-Meier recurrence-free survival curve of the Low-risk group was significantly better than the High-risk group (Figure 5, Wilcoxon test: p = 0.00006, log-rank test: p = 0.00029).

The best prediction models generated from only the clinical data ($\overline{\text{AUROC}}=0.6835$), T-miRs data ($\overline{\text{AUROC}}=0.7152$), and N-miRs data ($\overline{\text{AUROC}}=0.7530$) were obtained when 2 PCs, 6

Table 3. Recurrence-related principal components and correlated clinical factors.

		Cox proportional hazard model			
Rank	**Principal components**	**hazard ratio**	**p-value**	**Notable correlated clinical factors**	**p-value**
1	PC3	0.9592	0.0171	serum, AFP*	<0.0001
				serum, total-bilirubin*	0.0009
				HBV antigen§	0.0020
2	PC16	0.9044	0.0207	platelet*	0.0040
				Max diameter of tumor*	0.0135
				T-factor (clinical)**	0.0202
3	PC1	1.0335	0.0244	serum, PIVKA-II*	0.0018
				gender§	0.0398
4	PC4	1.0514	0.0246	HCV antibody§	0.0002
				serum, AST*	0.0037
				platelet*	0.0071
5	PC5	0.9591	0.0434	capsule formation (pathological)§	<0.0001
				presence of liver cirrhosis§	0.0042
				ICG-R15*	0.0198

*: continuous variables,
**: category variables,
§: dichotonized variables.
The p-values of correlation between PCs and clinical factors were calculated by Pearson's correlation analysis, Kruskal-Wallis test, and t-test for continuous, category, and dichotonized variables, respectively.
doi:10.1371/journal.pone.0016435.t003

PCs, and 10 individual microRNAs was used. The overall best prediction model predicts recurrences significantly better than these three models (paired t-test: $p<0.00001$). In addition, the $\overline{\text{AUROC}}$ of the N-miRs dataset was also significantly higher than that of T-miRs dataset. As shown in Figure 4, the AUROCs of the T-miRs models gradually decreased over the time course between 6 months and 5 years (Pearson's p-value <0.0001), which indicates that the T-miRs can predict early recurrences better than late recurrences. In contrast, the AUROCs of the N-miR models gradually elevated, which suggests that N-miRs can predict late recurrences better than early recurrences (Pearson's p-value <0.0001).

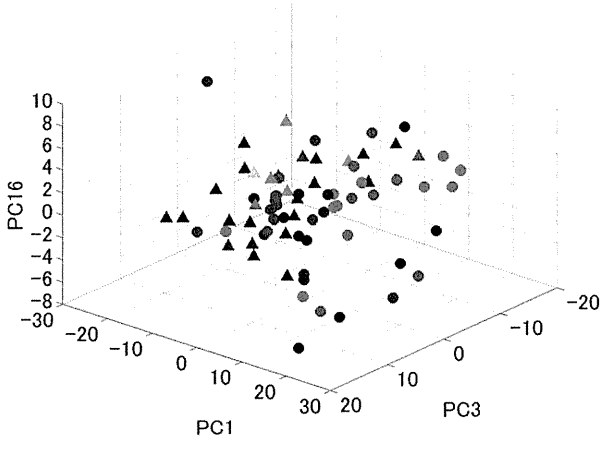

Figure 2. Three-dimensional scatter plot of PCA. The x-, y-, and z-axes represent the top-3 ranked PCs (PC3, PC16 and PC1). The color graduation scale from green, black to red represent short, intermediate, and long recurrence-free survival, respectively. The closed circles, and closed triangles correspond to complete and censored cases, respectively. Patients with poor outcomes tend to be in the right-lower side from this point of view, whereas patients with good outcomes tend to be in left-upper side.
doi:10.1371/journal.pone.0016435.g002

Contribution analysis of microRNAs in the best prediction model

The best overall model was constructed with the PCA and CoxPH model. Since the coefficients of the CoxPH model were for PCs not for individual microRNAs, it is difficult to determine how much each microRNA contributes to this prediction model. In this study, we combine the coefficients of the PCA and CoxPH, and converted them to a hazard ratio formula by PC values into individual microRNAs expression values. As shown in the supplemental Description S1, the coefficient of the i-th microRNA can be expressed as $\sum_{j}^{n} b_j Cj_i$, where n, b_j, and Cj_i represent the number of PCs, the beta value of the j-th PC, and the coefficient of the i-th microRNA in the j-th PC, respectively. Table 4 shows the top-20 contributory microRNAs or Tumor/Non-tumor ratios (T/N ratios) that are positively and negatively correlated with HCC recurrence. Interestingly, the expressions of miR-96 in non-tumor tissues and miR-96 T/N ratio are the top ranked microRNAs that are positively and negatively associated with HCC recurrence, respectively. To understand how miR-96 plays biological roles regarding HCC recurrence, it is important to identify target genes of miR-96. In this study, we identified three genes, LRP6, FOXO1A, and MAP2K1, that meet several criteria, such as, 1) possessing cancer-related functions according to an ontology database, 2) having microRNA target sites predicted by Target Scan v.5.1 (www.targetscan.org/) in their 3′-UTR, 3) inverse correlation to miR-96 expression level in 146 samples (tumor and non-tumor paired samples derived from 73 patients), (Table S2). Furthermore, we also checked whether the miR-96 expression data by DNA chips was reliable or not. The expression data of

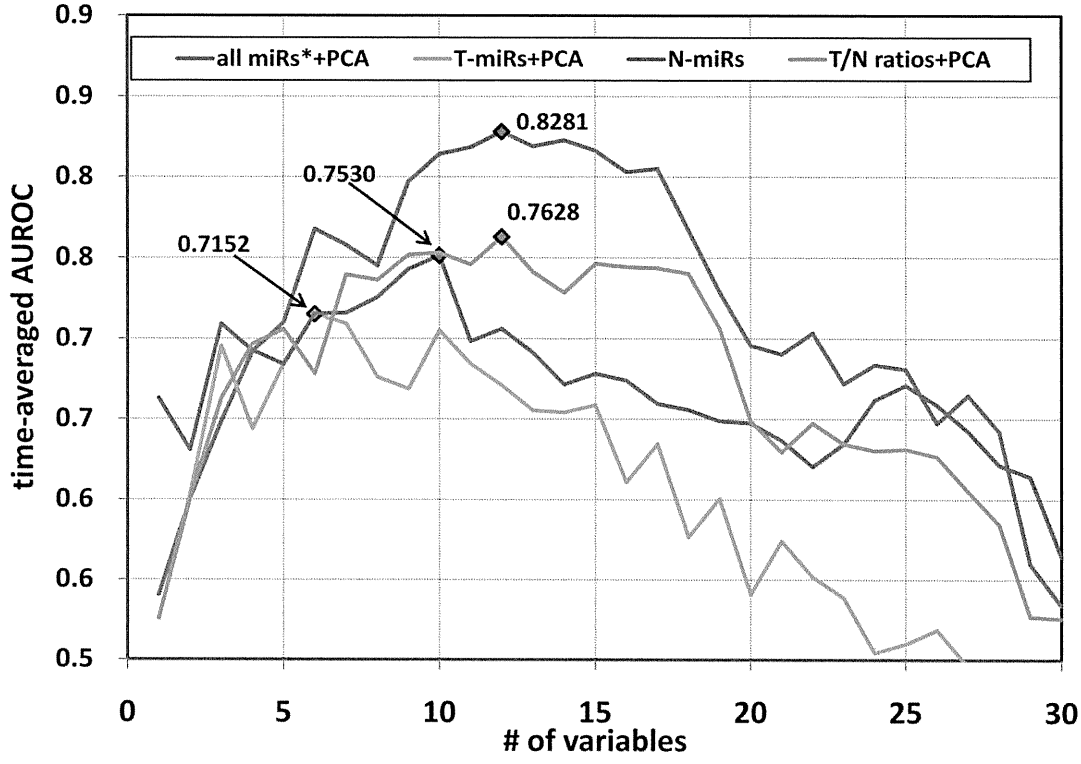

Figure 3. Changes in time-averaged AUROCs and the number of variables used for prediction model construction. The prediction models of HCC recurrence were constructed by the LOOCV method. The prediction accuracy for each model was evaluated by time-averaged AUROC between 6 months and 5 years after the operation. The $\overline{\text{AUROC}}$ were different depending upon the sample tissues, the inclusion or exclusion of PCA, and the number of variables used for constructing the prediction models. The best prediction accuracy was achieved when the model was construct using top-twelve PCs data derived from all microRNA data (*: expression data of T-miRs and N-miRs, and T/N ratios). The best models using T-miRs, N-miRs, and T/N ratios were obtained from the top-6 PCs, top-10 microRNAs, and top-12 PCs, respectively.
doi:10.1371/journal.pone.0016435.g003

miR-96 by Taqman RT-PCR assay was significantly correlated with that by DNA chip analysis (Figure S2).

Differentially expressed microRNAs

Differentially expressed microRNAs between T-miRs and N-miRs are shown in Table S3, S4. Among 73 cases enrolled in this study, 4 patients had macroscopically normal and pathologically normal (n = 1) or slightly fibrotic (n = 3) liver tissues. We listed differentially expressed microRNAs compared to these four normal liver samples in Table S5. According to Table S3, S4, S5, miR-96 expression level was gradually elevated from normal liver, via non-tumor liver tissues with accompanied chronic change, to tumor tissues. We also listed differentially expressed microRNAs depending upon HBV/HCV status and tumor differentiation grade in Table S6, S7, S8. Furthermore, using univariate Cox proportional hazard model, we show microRNAs significantly associated with HCC recurrence in subgroups categorized by HBV/HCV status and tumor differentiation grade in Table S9, S10, S11, S12.

Discussion

In this study, we performed microRNA signature analysis and developed a mathematical model to predict HCC recurrence in patients within the Milan Criteria and with mild liver cirrhosis (i.e., Child-Pugh A/B). To date, there are many microarray-based studies [18–21] that predict the outcomes of HCC patients. However, our study is the first microarray-based study that focuses on a potential population of patients for future salvage transplantation, and that underwent liver resection and fulfill the Milan Criteria.

Clinical significance of HCC recurrence prediction for patients within the Milan Criteria

HCC patients who satisfy the Milan Criteria and who have sufficient liver function have two potential curative therapeutic options: liver resection and orthotopic liver transplantation. However, both options have advantages and disadvantages. Therefore, a compromised option of liver resection plus salvage liver transplantation seems reasonable. Even taking this option, recurrent tumors must be detected in the early phase; otherwise, the benefits of salvage transplantation would be diminished. Performing intensive follow-ups for all LR patients is not feasible. Therefore, a strategy of more detailed follow-ups for patients with higher risk is necessary. This prediction model will be a helpful tool to stratify these patients.

In this study, we obtained a relatively high prediction accuracy ($\overline{\text{AUROC}}$ = 0.8281) using a combined dataset of T-miRs and N-miRs. Previously, many prediction models of HCC outcomes have been reported. However, it is very difficult to compare the prediction accuracy to other models, because the target population in the HCC patients from this study was different from those in other reports.

Significance of microRNA profile in tumor and non-tumor tissues

In this analysis, the prediction efficiency constructed using the N-miRs dataset was better than that constructed using the T-miRs. It is reasonable, because there are more recurrence-related microRNAs in the N-miRs than in the T-miRs, according to univariate CoxPH model analyses (Table 2). Previously, we reported that co-existing cirrhosis was associated with a higher

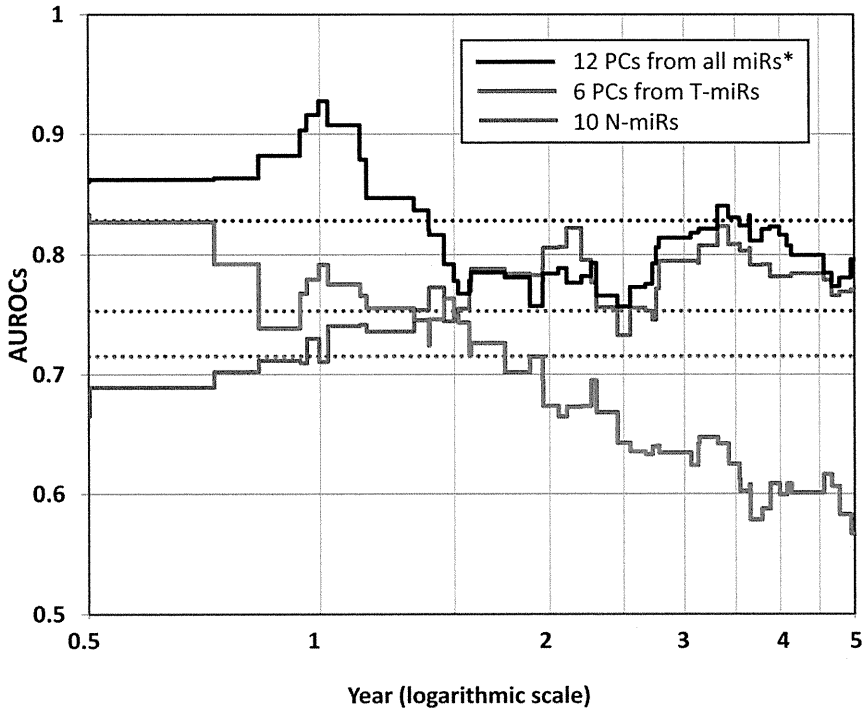

Figure 4. The AUROC changes of the best prediction model between 6 months and 5 years. In general, the prediction accuracy depends upon the time point used to evaluate the prediction accuracy of the survival curve. Thus, we adopted $\overline{\text{AUROC}}$ as an index of prediction accuracy for the survival curve. To cover both early and late recurrences, we calculated the $\overline{\text{AUROC}}$ between 6 months and 5 years. The black step graph shows the changes in the AUROCs for the overall best prediction model ($\overline{\text{AUROC}} = 0.8281$). The red and blue step graphs represent the changes of AUROCs of the best models using T-miRs and N-miRs datasets. The dotted lines of each color correspond to the $\overline{\text{AUROC}}$ for each step graph. This prediction model using T-miRs can predict early recurrences better, whereas the model using N-miRs is better for late recurrences.
doi:10.1371/journal.pone.0016435.g004

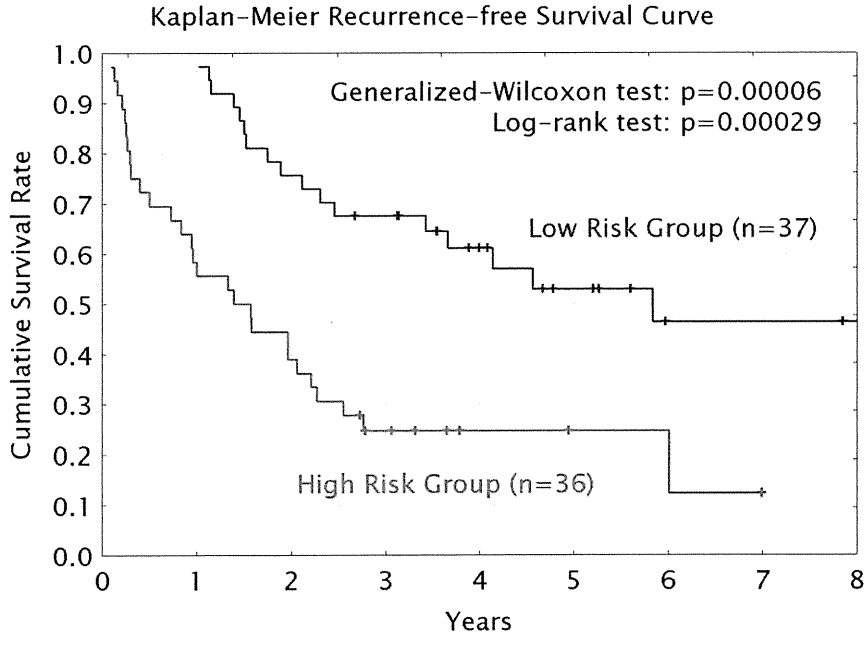

Figure 5. Kaplan-Meier cumulative recurrence-free survival curves. According to the predicted recurrence-free survival rate, the patients were stratified as low (n = 37) and high (n = 36) risk groups. The recurrence-free survival of the low risk group was significantly better than that of high risk group by both a generalized-Wilcoxon test and the log-rank test.
doi:10.1371/journal.pone.0016435.g005

Table 4. Contribution analysis of individual microRNAs in the overall best prediction model.

	microRNAs positively associated with recurrence				microRNAs negatively associated with recurrence			
Rank	miR name	Tissue type	Coefficient	95%CI†	miR name	Tissue type	Coefficient	95%CI†
1	miR-96 §	N	0.1349	(0.1259~0.1449)	miR-96	T/N ratio	−0.0865	(−0.0941~−0.0793)
2	miR-139-5p	T/N ratio	0.0750	(0.0661~0.0850)	miR-374b	T/N ratio	−0.0785	(−0.0861~−0.0710)
3	miR-139-5p	T	0.0727	(0.0646~0.0815)	miR-182	T/N ratio	−0.0604	(−0.0659~−0.0549)
4	miR-126*	T	0.0676	(0.0620~0.0737)	miR-378 §	N	−0.0561	(−0.0612~−0.0511)
5	miR-142-3p	T	0.0673	(0.0599~0.0749)	miR-193b	T/N ratio	−0.0543	(−0.0600~−0.0493)
6	miR-142-3p	T/N ratio	0.0659	(0.0575~0.0754)	miR-193b	T	−0.0539	(−0.0596~−0.0483)
7	miR-362-3p	T	0.0596	(0.0538~0.0659)	miR-214	T/N ratio	−0.0535	(−0.0585~−0.0489)
8	miR-374b	N	0.0563	(0.0499~0.0629)	miR-125b §	T	−0.0522	(−0.0569~−0.0479)
9	miR-10b	T	0.0548	(0.0482~0.0616)	miR-125b	T/N ratio	−0.0521	(−0.0565~−0.0483)
10	miR-200a	N	0.0544	(0.0486~0.0599)	miR-99b	T/N ratio	−0.0517	(−0.0564~−0.0474)
11	miR-224	N	0.0530	(0.0466~0.0599)	miR-1202 §	N	−0.0515	(−0.0584~−0.0451)
12	miR-483-3p	T	0.0529	(0.0459~0.0602)	miR-18b	T/N ratio	−0.0513	(−0.0590~−0.0440)
13	miR-200a	T	0.0527	(0.0477~0.0580)	miR-365	T/N ratio	−0.0511	(−0.0573~−0.0454)
14	miR-1202	T/N ratio	0.0507	(0.0441~0.0574)	miR-100	T/N ratio	−0.0506	(−0.0559~−0.0456)
15	miR-96	T	0.0484	(0.0423~0.0543)	miR-365	T	−0.0504	(−0.0563~−0.0445)
16	miR-665	T/N ratio	0.0474	(0.0413~0.0534)	miR-210	T	−0.0502	(−0.0567~−0.0440)
17	miR-1274a	T/N ratio	0.0472	(0.0428~0.0518)	miR-100 §	T	−0.0500	(−0.0547~−0.0459)
18	miR-10b	T/N ratio	0.0471	(0.0408~0.0533)	miR-214	T	−0.0491	(−0.0544~−0.0443)
19	miR-665	T	0.0469	(0.0411~0.0528)	miR-378 §	T	−0.0489	(−0.0536~−0.0444)
20	miR-1228	T/N ratio	0.0446	(0.0398~0.0500)	miR-182	T	−0.0476	(−0.0534~−0.0419)

Positive and negative coefficients indicates that higher and reduced expression of microRNA is associated with recurrence, respectively.
§: overlapped microRNAs in Table 2.
†: CI, confidence interval, calculated by 1000 times bootstrap resampling.
doi:10.1371/journal.pone.0016435.t004

recurrence rate after hepatic resection of HCC within the Milan Criteria. This finding suggests that recurrences due to the dissemination of primary tumors cells occur more often within the initial few years after resection, and that late recurrences in cirrhotic livers are likely attributable to multicentric de novo carcinogenesis rather than dissemination of the primary tumor. In this study, as shown in Figure 4, the T-miR models can predict early recurrences better than late recurrences, whereas the N-miR models can predict late recurrences better than early recurrences. This finding suggests that the T-miR profile would represent the malignant potential of primary tumors, and would be associated with the presence of dissemination and the consequent early recurrence, and that the N-miR profile would reflect the accumulation of genome abnormalities (the 'field effect') in the remaining non-cancerous liver cells, and would be associated with multicentric late recurrence. Recently, several papers have reported that an abnormal mRNA expression profile in non-cancerous tissues is associated with HCC recurrence [21,29,30]. Moreover, our previous clinical study showed that co-existing cirrhosis correlated with the prognosis and recurrence of HCC within the Milan Criteria [8]. Therefore, our finding derived from the microRNA profile also supports the concept of early and late recurrence that these previous reports have proposed.

HBV infection, miR-96, and HCC Recurrence

The contribution analysis of microRNAs in the best prediction model demonstrated that miR-96 in non-tumor tissues was the most strongly associated with HCC recurrence. Previously, miR-96 was identified as HBV infection-related microRNA[31]. In this study, HBV infection and HBV-related PC3 were significantly correlated with HCC recurrence, according to the univariate CoxPH model (Table 2–3). Thus, it was reasonable that miR-96 was identified as a recurrence-related microRNA. In a supplement analysis, we identified three genes, LRP6, FOXO1A, and MAP2K1, that meet several criteria, described in result section. Among them, the TargetScan predicted that FOXO1A has the highest context score (an index for strength of bond between mature microRNA and target sites to miR-96. Despite a strong inverse correlation with miR-96 expression, LRP6 and MAP2K1 were predicted to have the relatively lower context scores than FOXO1A. Taken together, FOXO1A would be the most important HCC-related target gene of miR-96 microRNAs. This finding was concordant with a previous report[32].

Time-averaged AUROCs as an index for survival prediction accuracy

The CoxPH model can analyze data containing censored cases, and can predict the survival curves of test cases using a baseline survival curve by calculating a hazard ratio. However, it is difficult to evaluate the prediction accuracy of CoxPH models. Usually, analysts stratify the patients according to the CoxPH model predictions, and then compare the difference between groups using a generalized-Wilcoxon or log-rank tests, or calculate the sensitivity, specificity, or AUROC at a given time point, such as the 2-year survival. However, the prediction accuracy of survival models depends upon stratification criteria of the patients and the selection of a prediction time point. Therefore, the prediction accuracy of survival models may be

under- or over-estimated. Thus, we proposed time-averaged AUROC as a new evaluation index for the prediction efficiency of the CoxPH model, which will be a robust index.

Future prospects regarding clinical application of microarray technology

The MAQC project was initiated by the U.S. FDA, and the second phase (MAQC-II) is currently in progress [33]. Its aims are to assess the capabilities and limitations of microarray-based predictive models, and to reach a consensus for the development and validation of microarray-based predictive models for personalized medicine. Although reports from MAQC-II have not been published yet, their reports will have a great impact on finalizing a draft guideline of IVDMIA. Prior to finalizing the IVDMIA guideline by the U.S. FDA, the FDA have already cleared two microarray-based IVDMIA devices, MammaPrint™ and Pathwork Tissue Origin Test™. In addition, OncoTypeDX®, a RT-PCR-based IVDMIA, is widely used because health insurance companies have adopted it as a criterion for insurance payment. However, a microRNA-based IVDMIA device has not been developed and approved yet. MicroRNA can be detected even in formalin-fixed paraffin-embedded specimens [34], or remote fluid samples such as blood[35], because of their stability. Therefore, microRNAs are thought to be good biomarkers. The progress in this study will be fundamental for the future application of microRNA-microarray based IVDMIA into the clinical field. However, our prediction model was only internally validated. Therefore, prospective and external validation is necessary before it is introduced to put microRNA microarray into practical use.

Supporting Information

Description S1 Details of analysis procedures were described.
(DOC)

Figure S1 A heatmap and unsupervised clustergram of microRNA expression in tumor and non-tumor tissues of HCC patients. This heatmap represents an overview of microRNA expression profile. The microRNA expression data was centered by 2 directions (i.e., by genes and patients). Red, green, and black represent high, low, and intermediate microRNA expression. Blue and yellow bars on the top of the heatmap represent non-tumor, and tumor tissues.
(DOC)

Figure S2 Correlation between DNA chip and Taqman data for miR-96 expression. DNA chip expression data for miR-96 were validated by Taqman microRNA assay. DNAchip data and Taqman data were significantly correlated ($p<0.0001$). Left: x-axis: DNA chip data in a log2 scale, y-axis: Taqman data in an arbitrary log2 scale. Right: x-axis: DNA chip data in a log2 scale, y-axis: Taqman data in a log2 scale.
(DOC)

Table S1 Variables in clinicopathological dataset.
(DOC)

Table S2 Putative miR-96 target genes which expression is inversely correlated with miR-96 expression. *: these values are provided by TargetScan v.5.1, **: rank of total context score among 787 putative miR-96 target genes predicted by TargetScan. †: Pearson's correlation coefficients and p-values, ‡: Pubmed hit count using key words of gene symbol and "HCC, liver cancer, hepatocellular carcinoma", accessed on Dec 26, 2010.
(DOC)

Table S3 Significantly up-regulated microRNAs in HCC tumor tissues compared to non-tumor tissues. Up-regulated microRNAs with $p<0.01$ are listed. T-miRs, N-miRs: mean values of each T-miR and NmiR expression in log2 scale, fold change: expression ratio of each T-miR compared with corresponding N-miR, p-value: p-values of paired T-test. Order of microRNA is sorted by fold-change.
(DOC)

Table S4 Significantly down-regulated microRNAs in HCC tumor tissues compared to non-tumor tissues. Down-regulated microRNAs with $p<0.01$ are listed. T-miRs, N-miRs: mean values of each T-miR and NmiR expression in log2 scale, fold change: expression ratio of each T-miR compared with corresponding N-miR, p-value: p-values of paired T-test. Order of microRNA is sorted by fold-change.
(DOC)

Table S5 Differentially expressed microRNA compared with normal liver tissues. Differentially expressed microRNAs with $p<0.05$ are listed. T-miRs, N-miRs: mean values of each T-miR and NmiR expression in log2 scale, fold change: expression ratio of each T-miR or N-miR compared with normal liver tissues ($n=4$), p-value: p-values of unpaired T-test. The miR order is sorted by fold-change.
(DOC)

Table S6 Differentially expressed microRNAs depending upon HBV status. *: p-values of Student's T-test. Differentially expressed microRNAs with $p<0.05$ are listed.
(DOC)

Table S7 Differentially expressed microRNAs depending upon HCV status. * p-values of Student's T-test. Differentially expressed microRNAs with $p<0.05$ are listed.
(DOC)

Table S8 Differentially expressed microRNAs depending upon cellular grade. *: p-values of one-way ANOVA test. Differentially expressed microRNAs with $p<0.05$ are listed.
(DOC)

Table S9 Recurrence related microRNAs in HBV-positive cases. Univariate Cox proportional hazard model identified microRNAs associated with poor (red) and better (blue) recurrent outcome, respectively. Top-twenty significant microRNAs with p-value <0.05 are listed. MicroRNAs (displayed in red) which hazard ratio is greater than 1 were correlated with frequent recurrence, and are potential oncomiRs. In contrast, microRNAs (shown in blue) with hazard ratio less than 1 were associated with good recurrence-free survivals, and would be a tumor-suppressor miRs.
(DOC)

Table S10 Recurrence related microRNAs in HCV-positive cases. Univariate Cox proportional hazard model identified microRNAs associated with poor (red) and better (blue) recurrent outcome, respectively. Top-twenty significant microRNAs with p-value <0.05 are listed. MicroRNAs (displayed in red) which hazard ratio is greater than 1 were correlated with frequent recurrence, and are potential oncomiRs. In contrast, microRNAs (shown in blue) with hazard ratio less than 1 were associated with good recurrence-free survivals, and would be a tumor-suppressor miRs.
(DOC)

Table S11 Recurrence related microRNAs in hapatitis virus-negative cases. Univariate Cox proportional hazard model identi-

fied microRNAs associated with poor (red) and better (blue) recurrent outcome, respectively. Top-twenty significant microRNAs with p-value <0.05 are listed. MicroRNAs (displayed in red) which hazard ratio is greater than 1 were correlated with frequent recurrence, and are potential oncomiRs. In contrast, microRNAs (shown in blue) with hazard ratio less than 1 were associated with good recurrence-free survivals, and would be a tumor-suppressor miRs.
(DOC)

Table S12 Recurrence related microRNAs in grade 1–2 HCC cases. Univariate Cox proportional hazard model identified microRNAs associated with poor (red) and better (blue) recurrent outcome, respectively. Top-twenty significant microRNAs with p-value <0.05 are listed. MicroRNAs (displayed in red) which hazard ratio is greater than 1 were correlated with frequent recurrence, and are potential oncomiRs. In contrast, microRNAs (shown in blue) with hazard ratio less than 1 were associated with good recurrence-free survivals, and would be a tumor-suppressor miRs.
(DOC)

Acknowledgments

We thank Ms. Takako Murai and Ms. Chizuko Hirano for their technical assistance, and Ms. Sawako Okamoto for proofreading this article.

Author Contributions

Conceived and designed the experiments: FS EH. Performed the experiments: FS KK AM S. Tsuchiya. Analyzed the data: FS AM TF. Contributed reagents/materials/analysis tools: FS EH S. Takizawa GT SU KS. Wrote the paper: FS EH.

References

1. Stewart B, Kleihues P (2003) World Cancer Report. Lyon: IARC Press.
2. Akriviadis EA, Llovet JM, Efremidis SC, Shouval D, Canelo R, et al. (1998) Hepatocellular carcinoma. Br J Surg 85: 1319–1331.
3. El-Serag HB, Mason AC (1999) Rising incidence of hepatocellular carcinoma in the United States. N Engl J Med 340: 745–750.
4. Taylor-Robinson SD, Foster GR, Arora S, Hargreaves S, Thomas HC (1997) Increase in primary liver cancer in the UK, 1979–94. Lancet 350: 1142–1143.
5. Mazzaferro V, Regalia E, Doci R, Andreola S, Pulvirenti A, et al. (1996) Liver transplantation for the treatment of small hepatocellular carcinomas in patients with cirrhosis. N Engl J Med 334: 693–699.
6. Figueras J, Jaurrieta E, Valls C, Ramos E, Serrano T, et al. (2000) Resection or transplantation for hepatocellular carcinoma in cirrhotic patients: outcomes based on indicated treatment strategy. J Am Coll Surg 190: 580–587.
7. Michel J, Suc B, Montpeyroux F, Hachemanne S, Blanc P, et al. (1997) Liver resection or transplantation for hepatocellular carcinoma? Retrospective analysis of 215 patients with cirrhosis. J Hepatol 26: 1274–1280.
8. Taura K, Ikai I, Hatano E, Yasuchika K, Nakajima A, et al. (2007) Influence of coexisting cirrhosis on outcomes after partial hepatic resection for hepatocellular carcinoma fulfilling the Milan criteria: an analysis of 293 patients. Surgery 142: 685–694.
9. Ito T, Takada Y, Ueda M, Haga H, Maetani Y, et al. (2007) Expansion of selection criteria for patients with hepatocellular carcinoma in living donor liver transplantation. Liver Transpl 13: 1637–1644.
10. Bartel DP (2004) MicroRNAs: genomics, biogenesis, mechanism, and function. Cell 116: 281–297.
11. Griffiths-Jones S (2004) The microRNA Registry. Nucleic Acids Res 32: D109–111.
12. Zamore PD, Haley B (2005) Ribo-gnome: the big world of small RNAs. Science 309: 1519–1524.
13. Kim VN, Nam JW (2006) Genomics of microRNA. Trends Genet 22: 165–173.
14. Lagos-Quintana M, Rauhut R, Lendeckel W, Tuschl T (2001) Identification of novel genes coding for small expressed RNAs. Science 294: 853–858.
15. Tsuchiya S, Okuno Y, Tsujimoto G (2006) MicroRNA: biogenetic and functional mechanisms and involvements in cell differentiation and cancer. J Pharmacol Sci 101: 267–270.
16. John B, Enright AJ, Aravin A, Tuschl T, Sander C, et al. (2004) Human MicroRNA targets. PLoS Biol 2: e363.
17. Lu J, Getz G, Miska EA, Alvarez-Saavedra E, Lamb J, et al. (2005) MicroRNA expression profiles classify human cancers. Nature 435: 834–838.
18. Ye QH, Qin LX, Forgues M, He P, Kim JW, et al. (2003) Predicting hepatitis B virus-positive metastatic hepatocellular carcinomas using gene expression profiling and supervised machine learning. Nat Med 9: 416–423.
19. Lee JS, Chu IS, Heo J, Calvisi DF, Sun Z, et al. (2004) Classification and prediction of survival in hepatocellular carcinoma by gene expression profiling. Hepatology 40: 667–676.
20. Iizuka N, Hamamoto Y, Oka M (2004) Predicting individual outcomes in hepatocellular carcinoma. Lancet 364: 1837–1839.
21. Hoshida Y, Villanueva A, Kobayashi M, Peix J, Chiang DY, et al. (2008) Gene expression in fixed tissues and outcome in hepatocellular carcinoma. N Engl J Med 359: 1995–2004.
22. Budhu A, Jia HL, Forgues M, Liu CG, Goldstein D, et al. (2008) Identification of metastasis-related microRNAs in hepatocellular carcinoma. Hepatology 47: 897–907.
23. Meng F, Henson R, Wehbe-Janek H, Ghoshal K, Jacob ST, et al. (2007) MicroRNA-21 regulates expression of the PTEN tumor suppressor gene in human hepatocellular cancer. Gastroenterology 133: 647–658.
24. Ito T, Tanaka E, Kadowaki T, Kan T, Higashiyama M, et al. (2007) An ultrasensitive new DNA microarray chip provides gene expression profiles for preoperative esophageal cancer biopsies without RNA amplification. Oncology 73: 366–375.
25. Sato F, Tsuchiya S, Terasawa K, Tsujimoto G (2009) Intra-platform repeatability and inter-platform comparability of microRNA microarray technology. PLoS One 4: e5540.
26. Liver Cancer Study Group of Japan a (2000) The General Rules for the Clinical and Pathological Study of Primary Liver Cancer. Tokyo: Kanehara & Co., Ltd.
27. Centeno BA, Enkemann SA, Coppola D, Huntsman S, Bloom G, et al. (2005) Classification of human tumors using gene expression profiles obtained after microarray analysis of fine-needle aspiration biopsy samples. Cancer 105: 101–109.
28. Bolstad BM, Irizarry RA, Astrand M, Speed TP (2003) A comparison of normalization methods for high density oligonucleotide array data based on variance and bias. Bioinformatics 19: 185–193.
29. Utsunomiya T, Shimada M, Imura S, Morine Y, Ikemoto T, et al. (2010) Molecular signatures of noncancerous liver tissue can predict the risk for late recurrence of hepatocellular carcinoma. J Gastroenterol 45: 146–152.
30. Simon F, Bockhorn M, Praha C, Baba HA, Broelsch CE, et al. (2010) Deregulation of HIF1-alpha and hypoxia-regulated pathways in hepatocellular carcinoma and corresponding non-malignant liver tissue-influence of a modulated host stroma on the prognosis of HCC. Langenbecks Arch Surg.
31. Ladeiro Y, Couchy G, Balabaud C, Bioulac-Sage P, Pelletier L, et al. (2008) MicroRNA profiling in hepatocellular tumors is associated with clinical features and oncogene/tumor suppressor gene mutations. Hepatology 47: 1955–1963.
32. Guttilla IK, White BA (2009) Coordinate regulation of FOXO1 by miR-27a, miR-96, and miR-182 in breast cancer cells. J Biol Chem 284: 23204–23216.
33. FDA US MicroArray Quality Control (MAQC). http://www.fda.gov/ScienceResearch/BioinformaticsTools/MicroarrayQualityControlProject/default.htm.
34. Wang H, Ach RA, Curry B (2007) Direct and sensitive miRNA profiling from low-input total RNA. Rna 13: 151–159.
35. Lodes MJ, Caraballo M, Suciu D, Munro S, Kumar A, et al. (2009) Detection of cancer with serum miRNAs on an oligonucleotide microarray. PLoS One 4: e6229.

Preoperative FDG-PET Predicts Recurrence Patterns in Hepatocellular Carcinoma

Koji Kitamura, Etsuro Hatano, Tatsuya Higashi, Satoru Seo, Yuji Nakamoto, Kenya Yamanaka, Taku Iida, Kojiro Taura, Kentaro Yasuchika, et al.

Annals of Surgical Oncology

ISSN 1068-9265
Volume 19
Number 1

Ann Surg Oncol (2012) 19:156-162
DOI 10.1245/s10434-011-1990-y

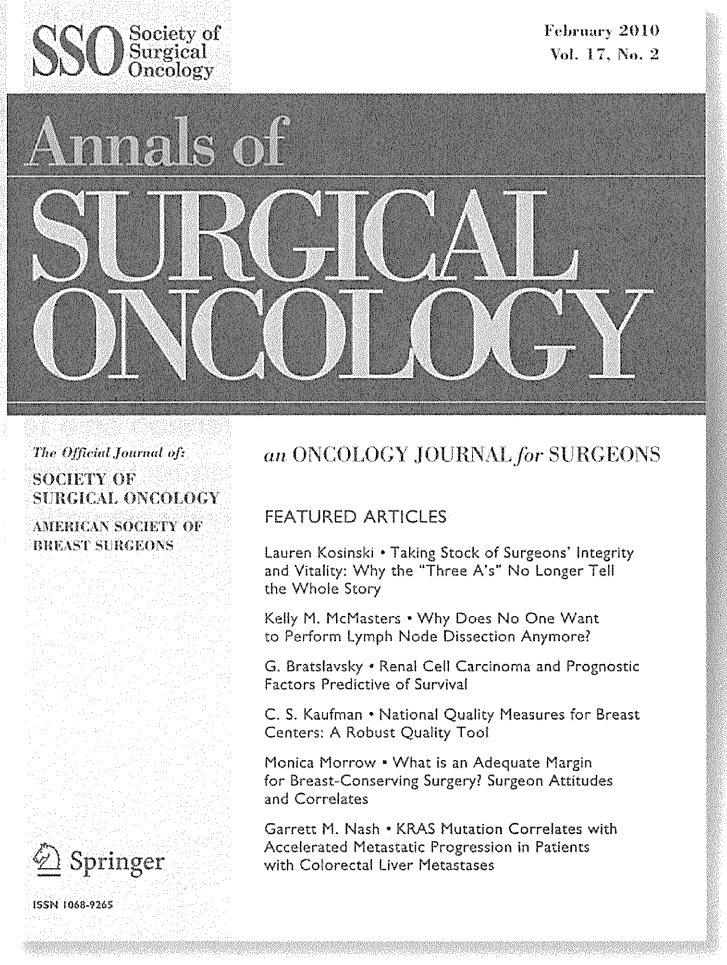

Springer